Longitudinal Shaping of Relativistic Electron Bunches with Applications to the Plasma Wakefield Accelerator

*R. Joel England, M. Hogan **

*G. Travish, J. B. Rosenzweig ***

** Stanford Linear Accelerator Center*
Advanced Accelerator Research Department
Menlo Park, CA

*** University of California, Los Angeles*
Particle Beam Physics Laboratory
Los Angeles, CA 90095

2009 Particle Accelerator Conference
May 7, 2009

Optimal Drive Beam Profile for Blowout Regime of PWFA

- PWFA: plasma wakefield accelerator
- electron beam-driven plasma waves
- acc. fields on order of multi-GeV/m
- acceleration of drive tail or witness bunch

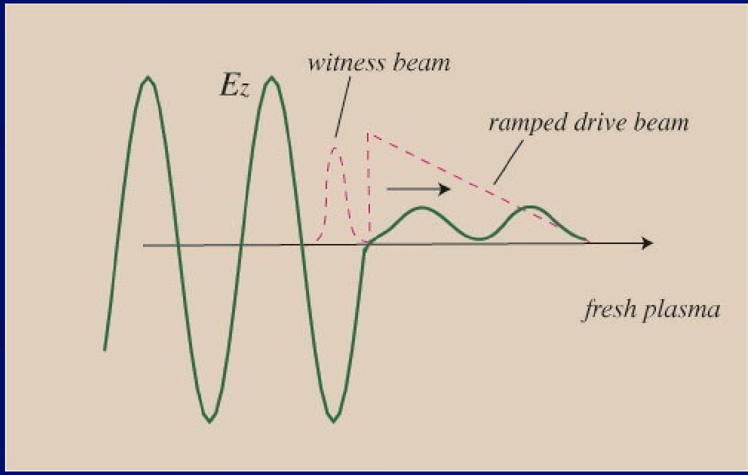

Chen, P., Su, J., and Dawson, J. SLAC PUB 3662 (1985).

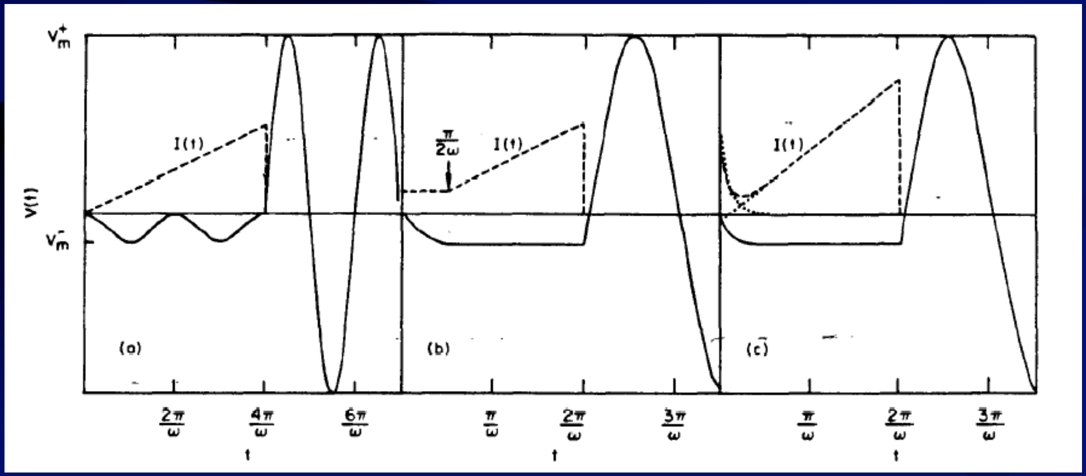

triangle **doorstep** **ideal**

Transformer Ratio:

$$E_+ = acc.field; E_- = decc.field$$

$$R = E_+ / E_- = k_p L_z$$

$$R > 2 \text{ if } L_z > 2k_p$$

Focus of this Talk

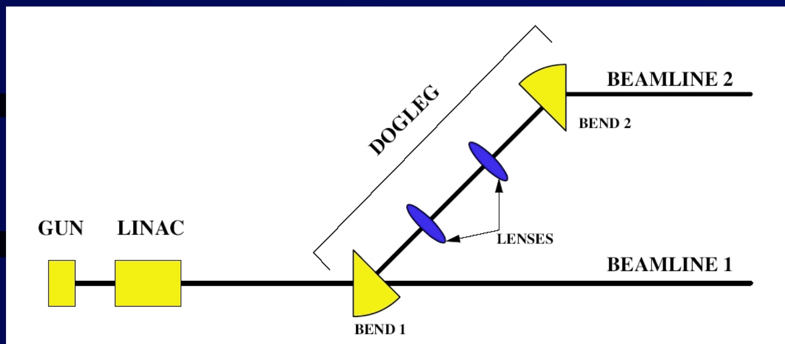

dogleg compressor

+

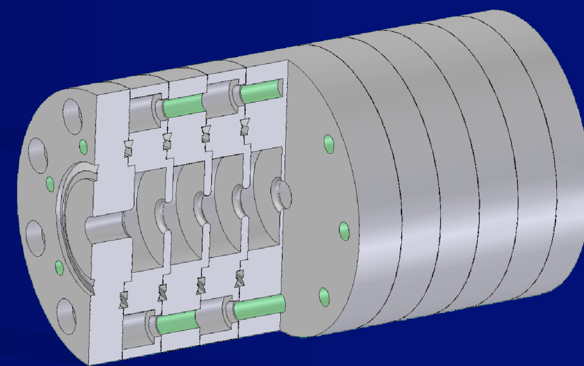

temporal diagnostic

=

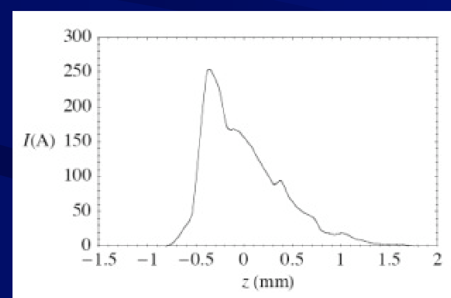

- Generation of electron beam with ramped current profile
- Temporal diagnostic with sub-ps resolution
  - transverse deflecting mode cavity
- Experimental verification of ramping mechanism

How Does a Dogleg Compress the Beam?

chicane

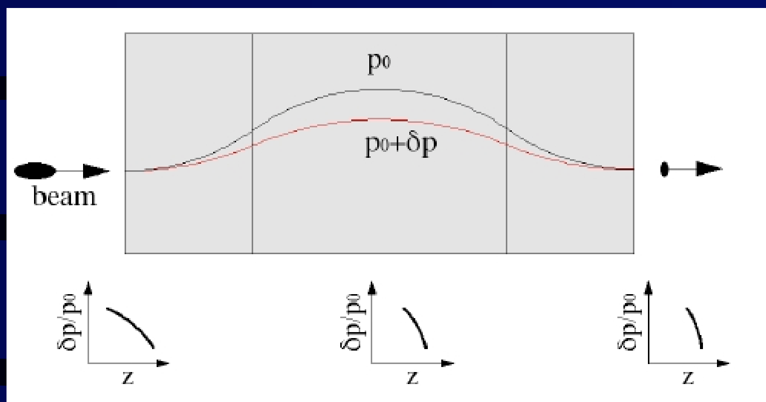

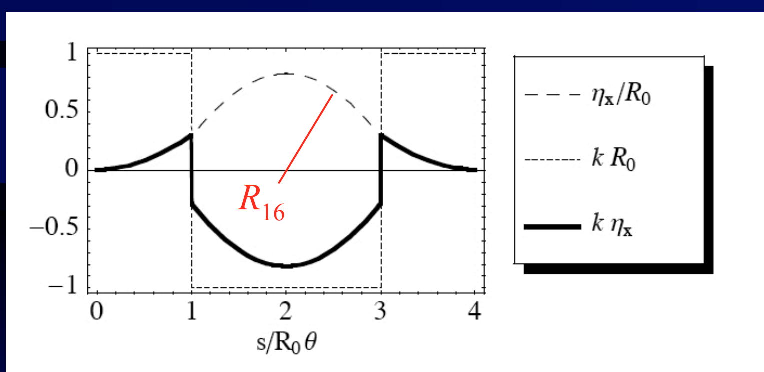

higher-energy particles travel a shorter path

$$R_{56} = \frac{\partial z}{\partial \delta} > 0$$ “positive longitudinal dispersion”

dogleg

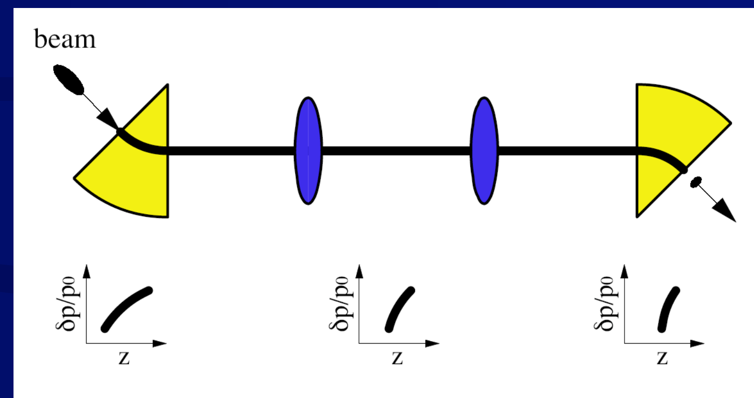

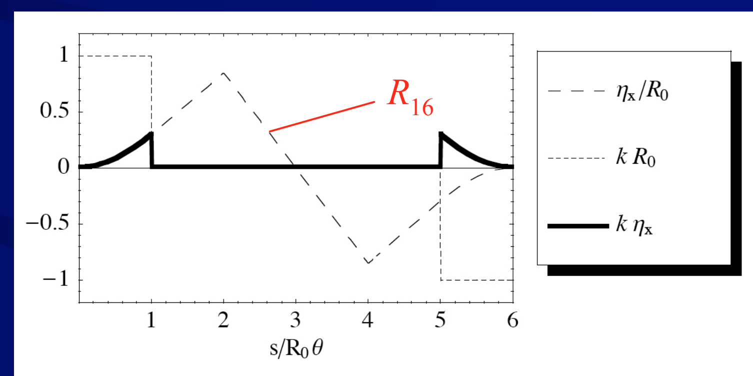

higher-energy particles travel a longer path

$$R_{56} = \frac{\partial z}{\partial \delta} < 0$$ “negative longitudinal dispersion”

Ramped Beam Mechanism

Artificial mathematical manipulation of a chirped particle distribution

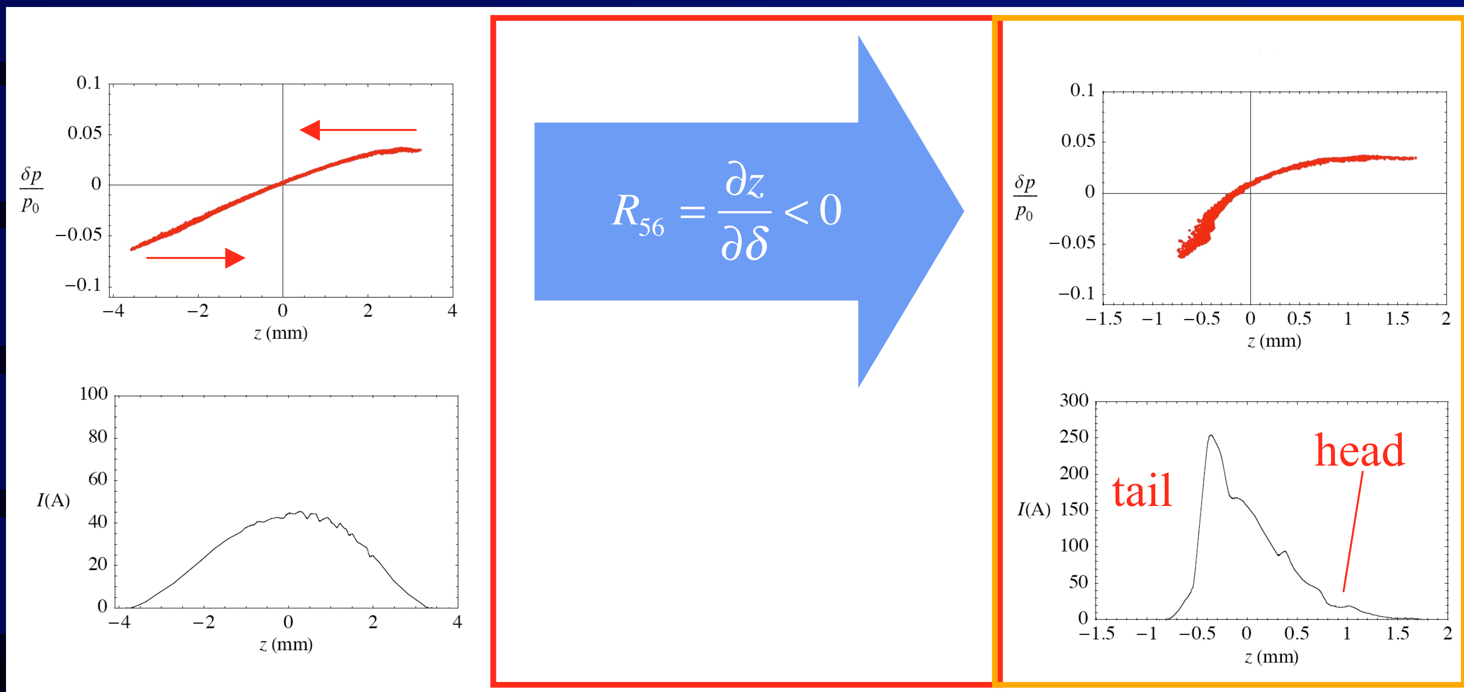

linear transformation: $z_f = z_0 + R_{56}\delta$

T_{566} arises from chromatic focusing errors in horizontally focusing quads and then grows in the subsequent drift sections (2nd order x-z correlation).

Solution: sextupole corrector magnets near the horizontally focusing quads.

Ramped Beam Mechanism

Artificial mathematical manipulation of a chirped particle distribution

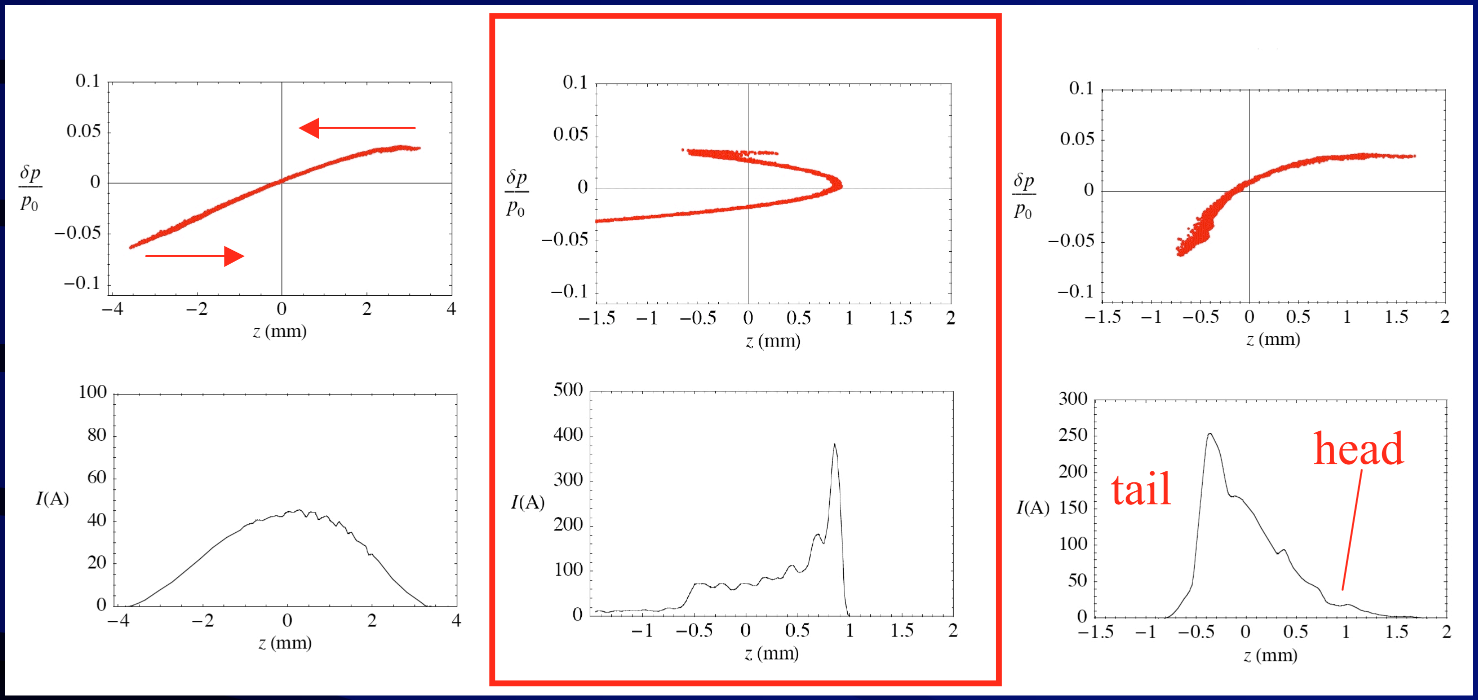

non linear transformation: $z_f = z_0 + R_{56}\delta + T_{566}\delta^2$

T_{566} arises from chromatic focusing errors in horizontally focusing quads and then grows in the subsequent drift sections (2nd order x-z correlation).

Solution: sextupole corrector magnets near the horizontally focusing quads.

UCLA Neptune Beamline

With Dogleg Compressor

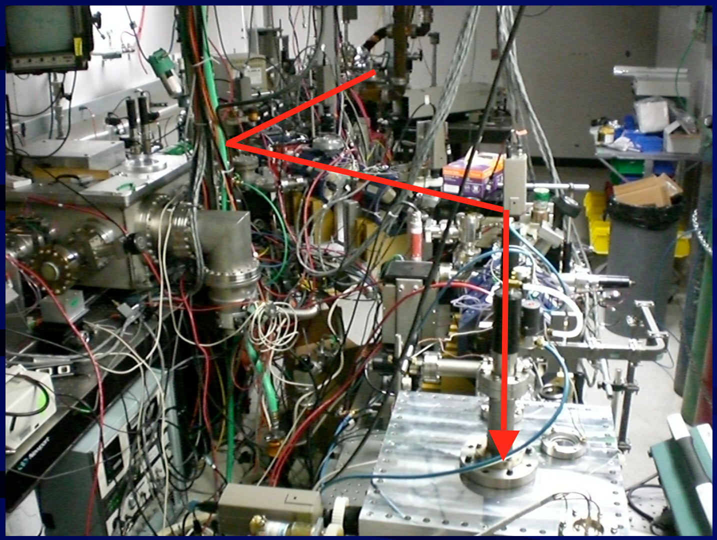

- Is a “dogleg” or dispersionless translating section.
- Half-chicane with focusing elements between the bends.
- Can be operated in a nondispersive mode with symmetric beta function and 2π betatron advance.
- Like a chicane, may be used as a bunch-length compressor.
- Nominal first order temporal dispersion (R_{56}=-5cm) is suitable for beam-shaping.
- Sextupoles required to compensate 2nd order longitudinal dispersion.

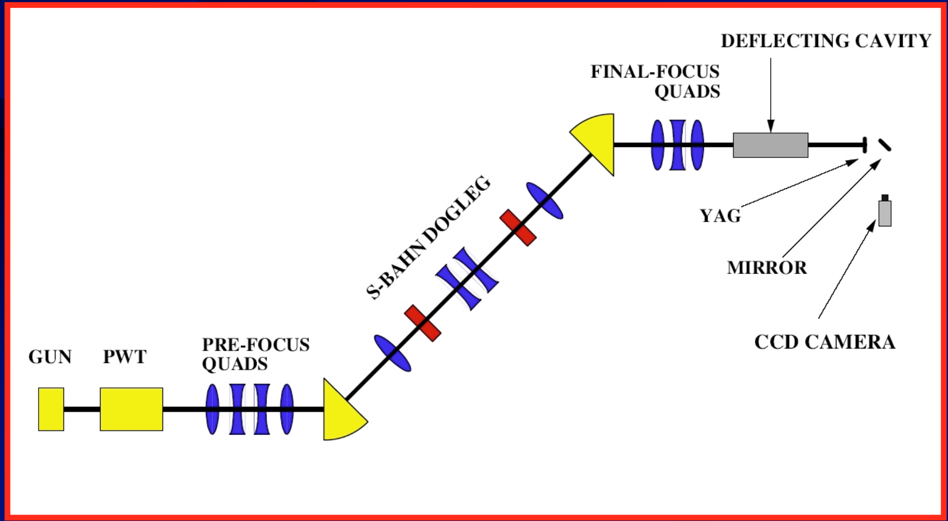

Neptune Dogleg Compressor

PARMELA Simulation Results: 1000 particles, 300pC

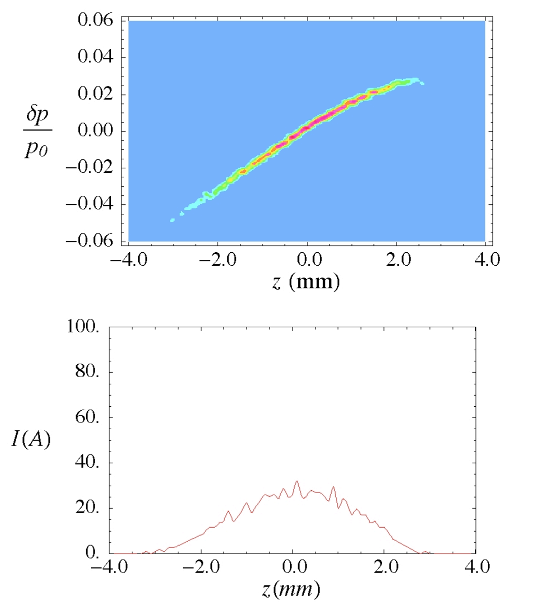

Initial

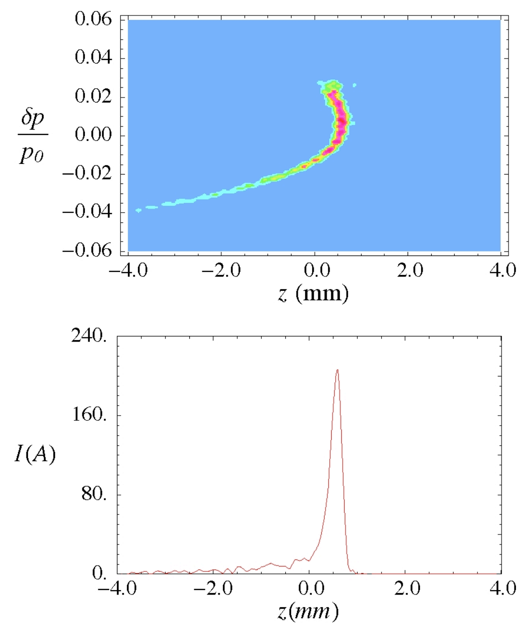

Final: Sextupoles Off

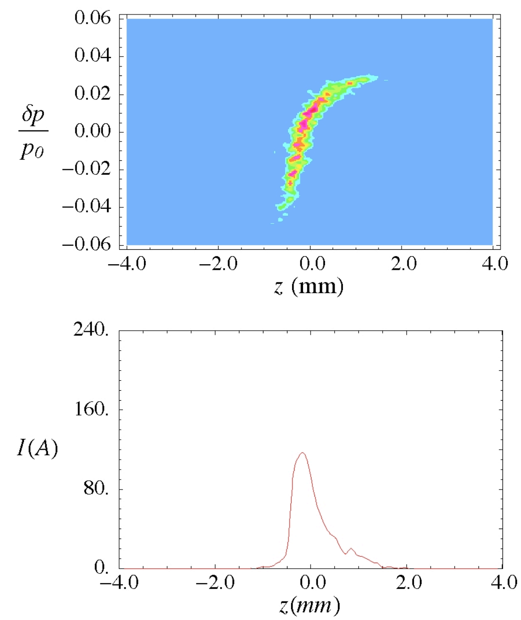

Final: Sextupoles On

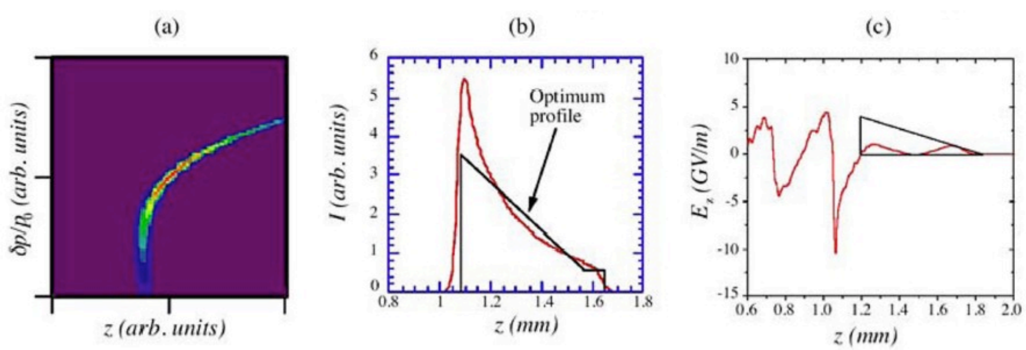

- 2D PIC Simulation
- 5 GeV/m gradients
- 6 nC drive beam w/ n_0=2e16 cm^{-3}

Neptune Dogleg Compressor

PARMELA Simulation Results: 1000 particles, 300pC

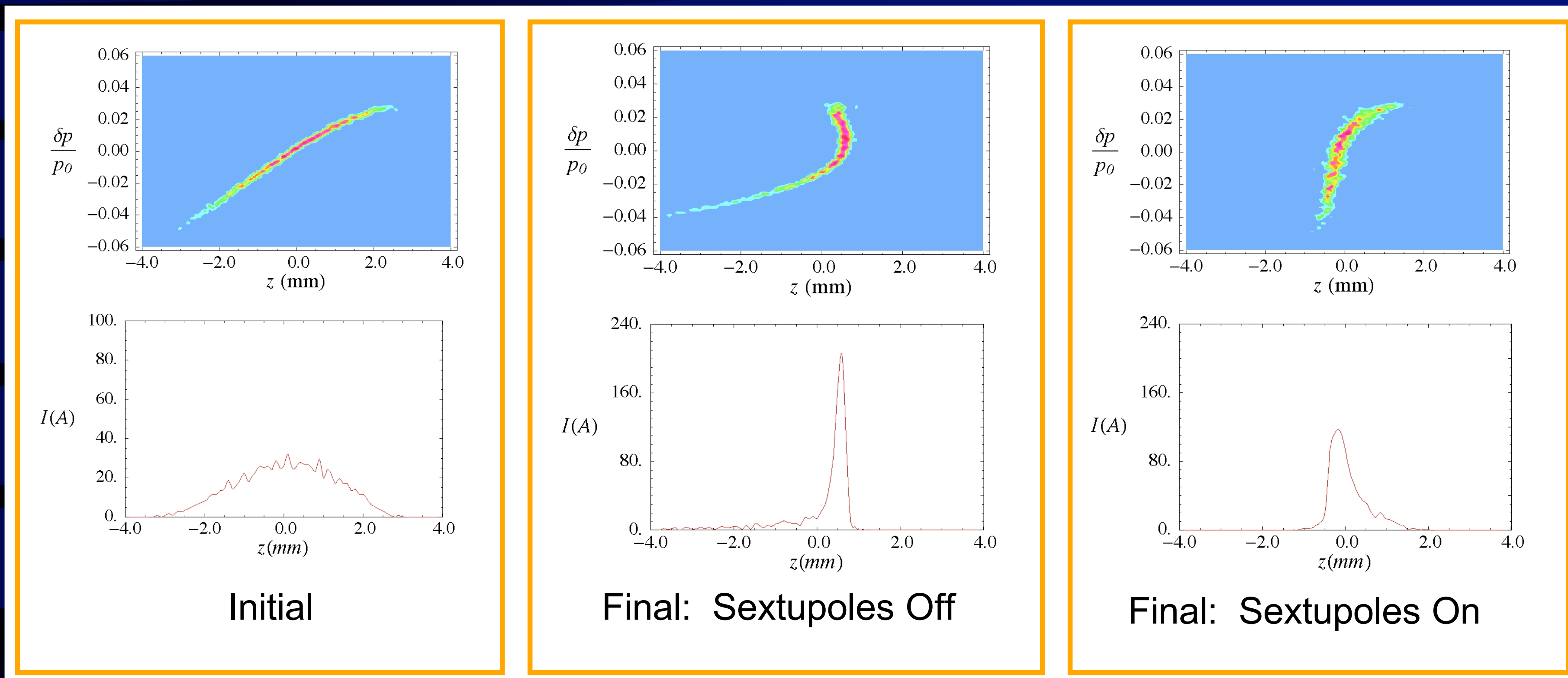

$\varepsilon_{x,N\ (\text{initial})}=4.9\ \mu\text{m}$

$\Delta\varepsilon_{x,N}=\underbrace{9.9\ \mu\text{m}}_{\text{space-charge}}+\underbrace{\overset{1.6}{\cancel{12.7}}}_{\text{nonlinear}}\mu\text{m}=\underbrace{\overset{11.5}{\cancel{22.6}}}_{\text{total}}\mu\text{m}$

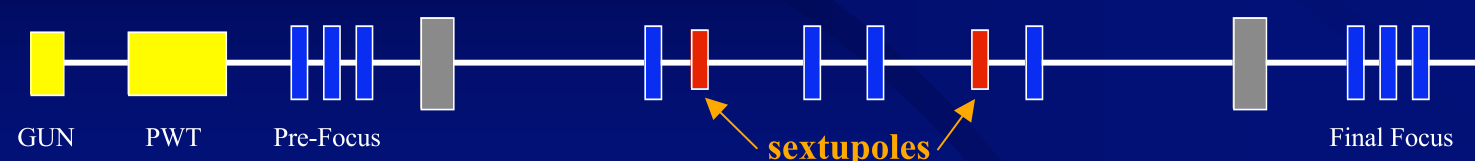

The UCLA Neptune Laboratory

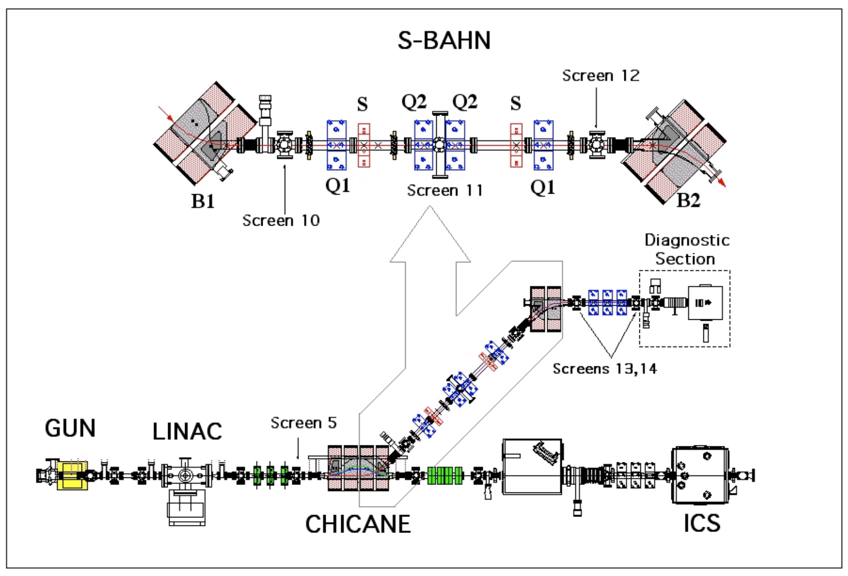

Beam Charge:	100pC ---> 500pC
Beam energy:	up to 15 MeV
Emittance:	ε_N = 4 mm mrad
Power Source:	18 MW Klystron
RF Frequency:	2.856 GHz
Cathode laser:	60 μJ at λ = 266 nm
Laser pulse length:	5-7 ps RMS

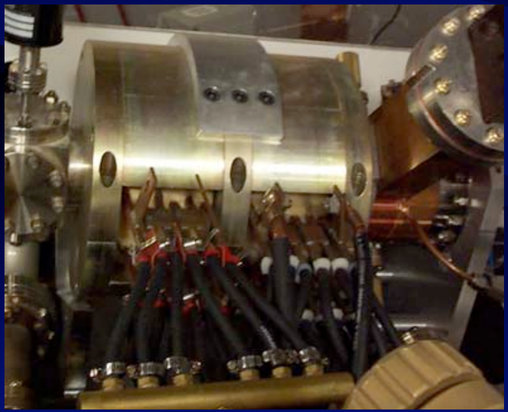

1.6-Cell Photoinjector

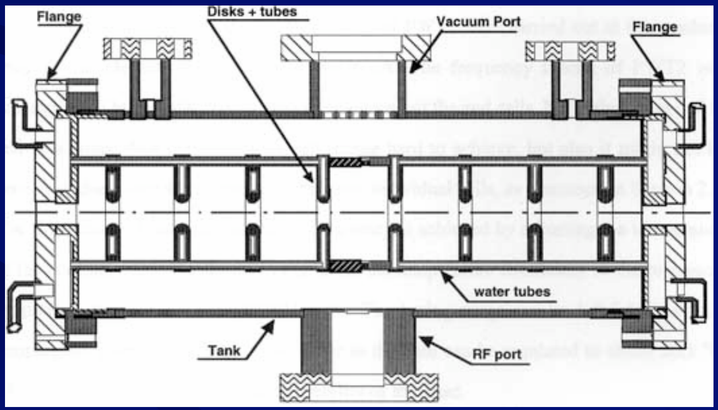

7&2/2 Cell PWT Linac

Coherent Transition Radiation Measurements of Compression

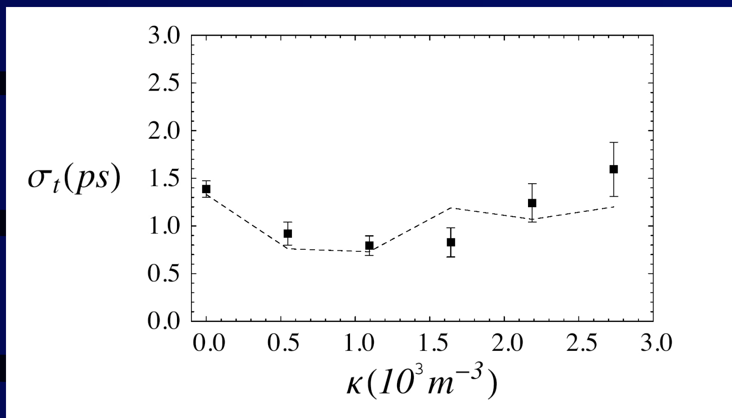

- Martin-Puplett CTR Interferometer
- Bunch length measurement by autocorrelation.
- Sub-picosecond resolution obtainable.

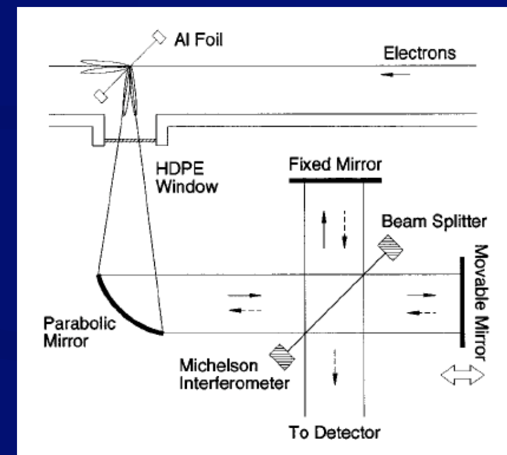

Simulations predict "ramped" beam occurs near point of maximum compression (κ=1094 m^{-3}).
Empirical CTR values obtained using method of [Murokh, et al., Nucl. Instr. Meth. Phys. Res. A, **410**, 452 (1998)].
Empirical analysis assumes a gaussian profile, which is not necessarily the case here.
Theoretical curve obtained from PARMELA + ELEGANT simulation, with autocorrelation algorithm.

PARMELA gun and linac 5000 macroparticles	→	ELEGANT prefocus and s-bahn 60% collimation	→	MATHEMATICA 1.interferogram reconstruction 2.triple-gaussian fit procedure

Coherent Transition Radiation Measurements of Compression

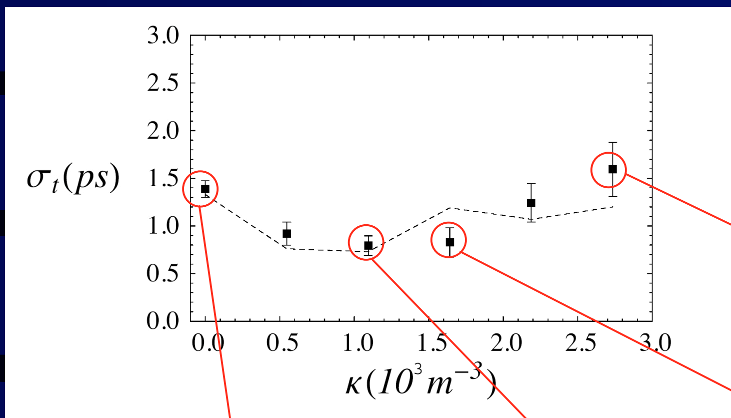

- Martin-Puplett CTR Interferometer
- Bunch length measurement by autocorrelation.
- Sub-picosecond resolution obtainable.

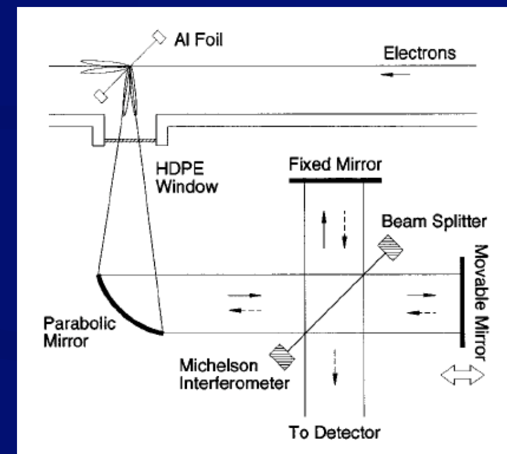

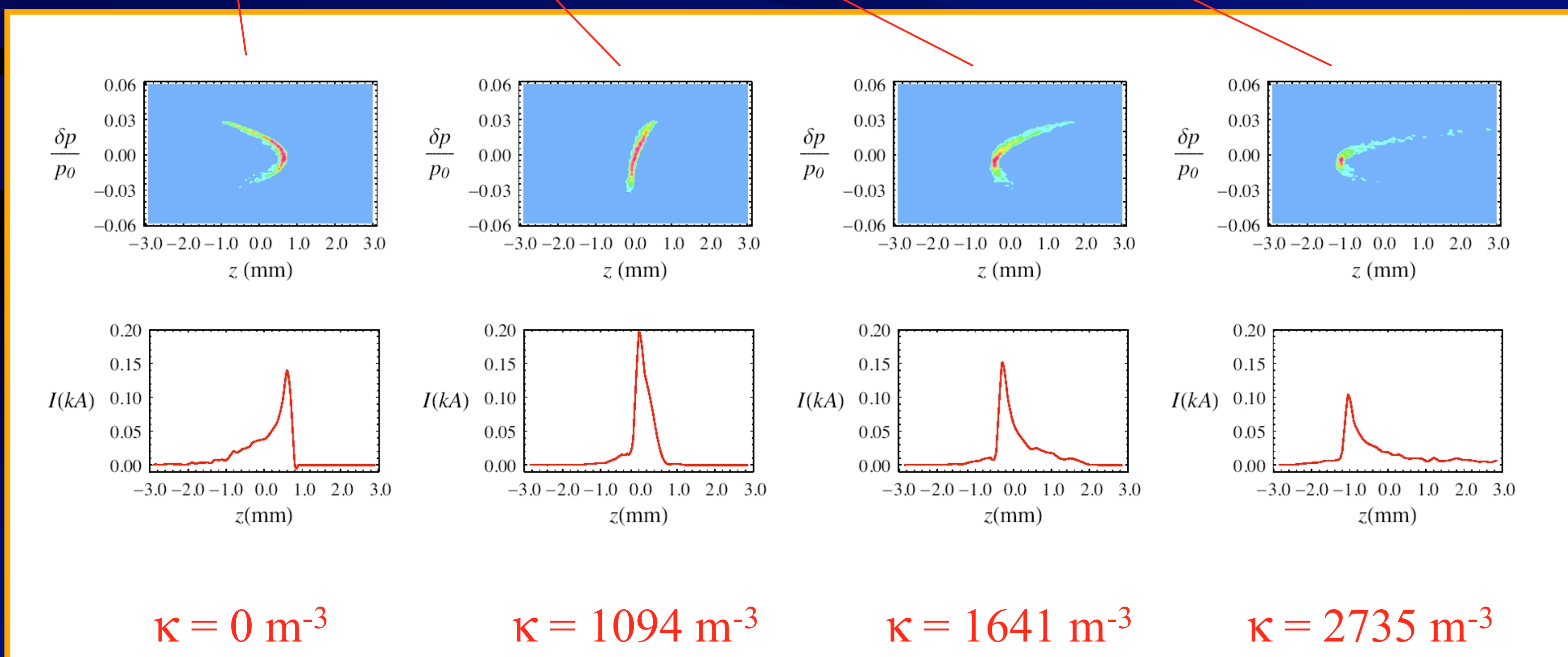

A Better Temporal Diagnostic

Deflecting Mode Cavity

Courtesy of D. Alesini

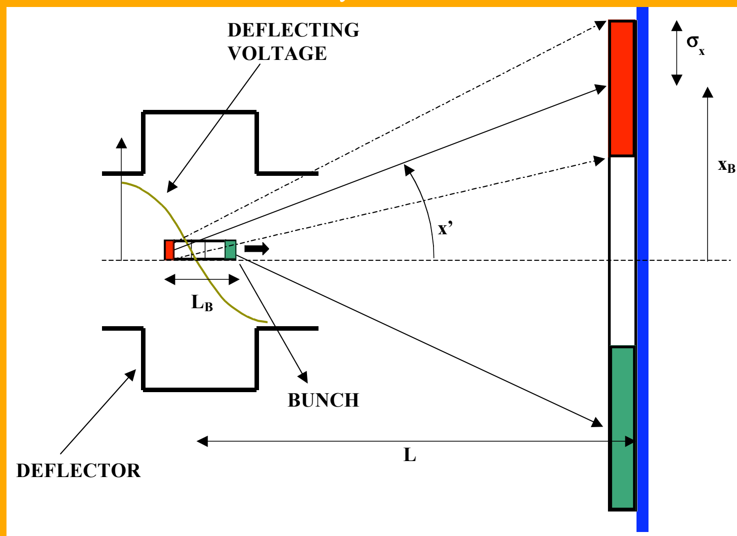

Lowest dipole mode is TM_{110}
Zero electric field on-axis (in pillbox approx.)
Deflection is purely magnetic
Polarization selection requires asymmetry

$$x' = \frac{\pi f_{RF} L_B \sqrt{2 P_{RF} R_\perp}}{cE/e}$$

$$x_B = \frac{\pi f_{RF} L L_B \sqrt{2 P_{RF} R_\perp}}{cE/e}$$

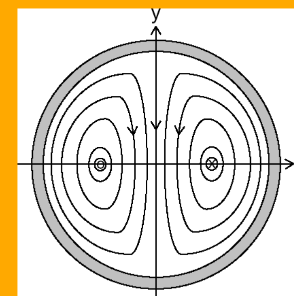

J.D. Fuerst, et. al., DESY Report CDR98, 1998

Pillbox Fields

$$E_z = E_0 J_1(\kappa r) e^{i\phi};$$

$$B_r = B_0 \frac{J_1(\kappa r)}{\kappa r} e^{i\phi};$$

$$B_\phi = i B_0 J_1'(\kappa r) e^{i\phi};$$

on axis
$\kappa r = 0$

$$E_z = 0;$$

$$B_x = \frac{B_0}{2};$$

$$B_y = i\frac{B_0}{2};$$

Deflecting Mode Cavity

Power and Resolution

screen deflection: $\sigma_{x,f} = \sqrt{\sigma_0^2 + \sigma_{def}^2}$ $\quad \sigma_{def} = 2\sigma_z L \dfrac{\pi V_\perp f}{cU/e}$

$$V_\perp >> V_{\min} = \frac{\sigma_{x,0} U/e}{L\pi\sigma_t f} \qquad \sigma_{t,\min} = \frac{\sigma_{x,0} U/e}{L\pi V_\perp f}$$

$$V_{\perp,design} = 3V_{\min} = 545\,kV \qquad \sigma_{t,\min} = 545\,fs$$

$$\Delta t = \frac{\sigma_0 \; U/e}{L\pi f R_\perp^{1/2}\sqrt{nP_{in}}}$$

$\sigma_{x,f}$ = beam size at screen with deflector on;

$\sigma_0 = 0.3mm$ = beam size at screen with deflector off;

$L = 43cm$ = drift from deflector to screen;

$f = 9.6GHz$ = RF frequency;

$V_\perp$ = deflecting voltage;

$R_\perp = 820k\Omega$ = transverse shunt impedance per cell;

P_{in} = input RF power;

$U = 12\,MeV$ = electron beam energy;

φ_0 = deflector injection phase = 0;

$\sigma_{t,\min}$ = minimum resolvable rms bunch length;

$\Delta x = 30\,\mu m$ = spatial resolution of screen & optics;

Δt = effective temporal resolution of deflector;

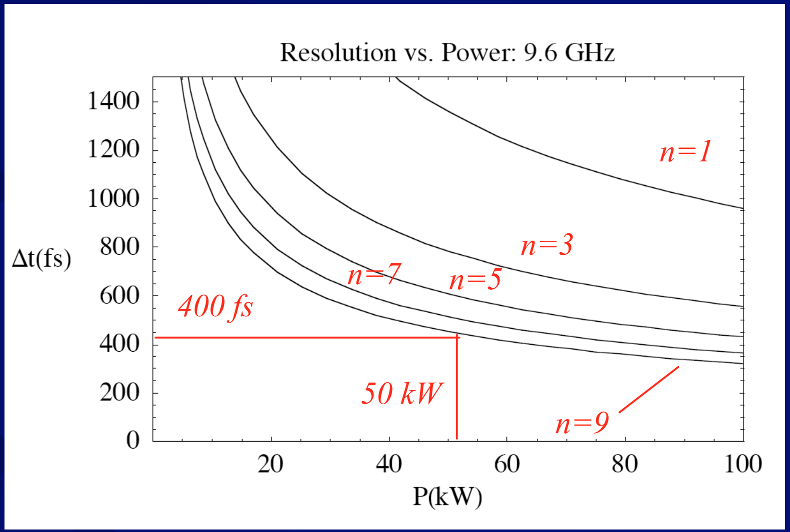

9 cells; 50 kW; 400 fs resolution

Overview of Design Process

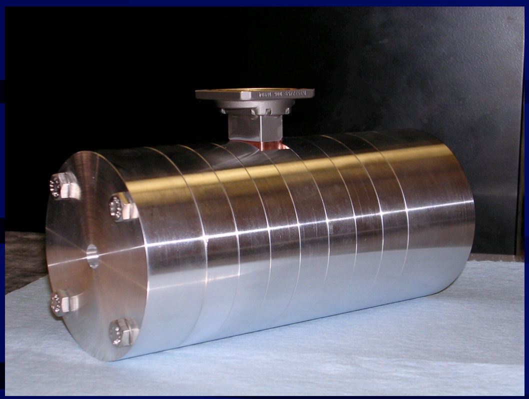

cold test prototype

Aluminum
9-cell
9.3 GHz
cold-test only
clamped
no polarization separation

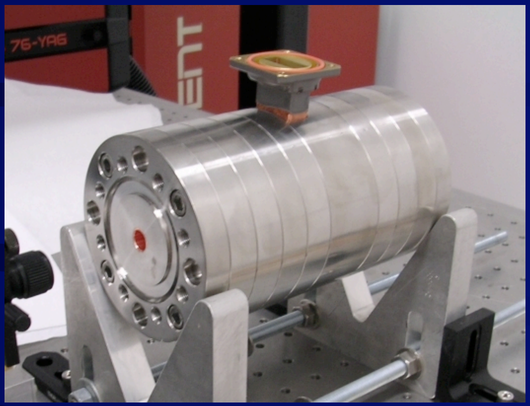

steel prototype

Steel with Cu coating
9-cell
9.5 GHz
cold-test only
cf flange design
no polarization separation

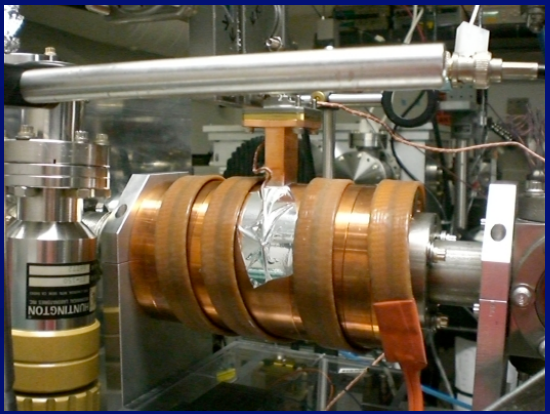

final design

GlidCop Al-15
9-cell
9.59616 GHz
tested up to 50kW peak pwr
conflat flange design
EDM’ed polarization holes

Deflecting Cavity Animations

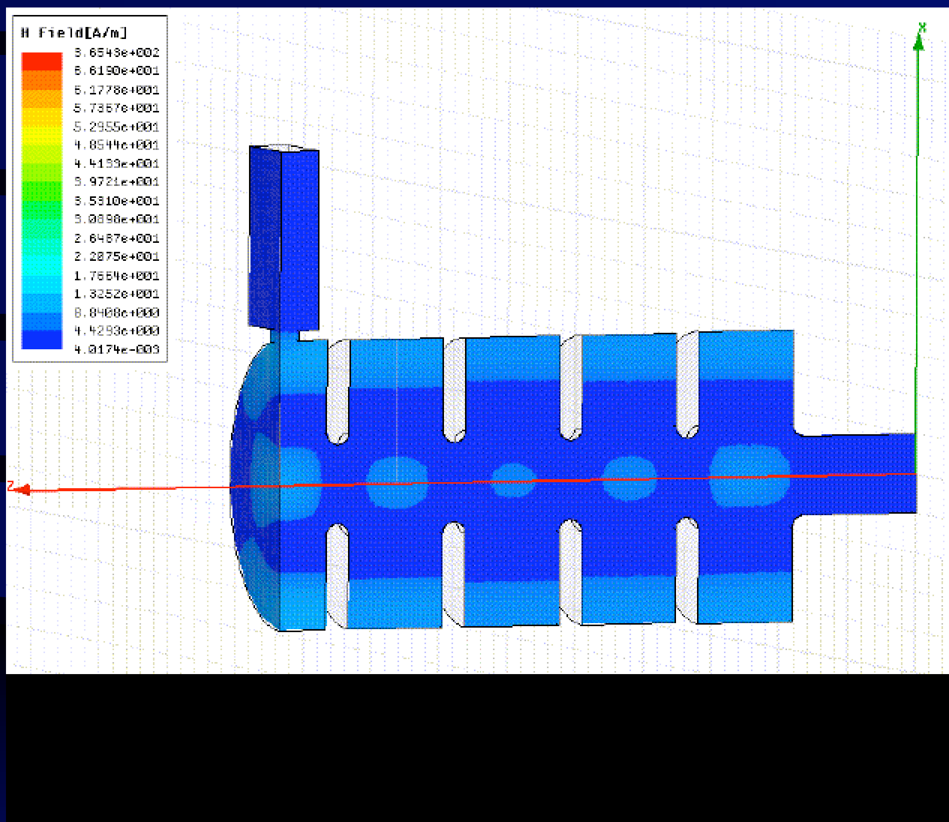

H-field complex magnitude

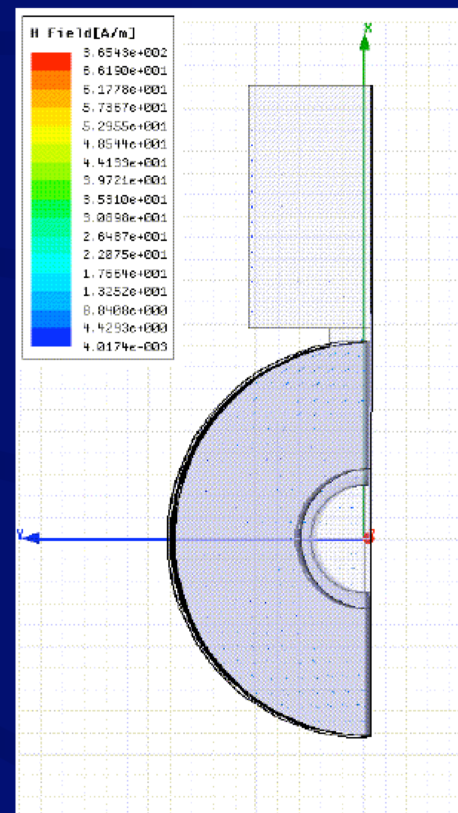

H-field vector plot

Deflecting Cavity: Polarization Separation

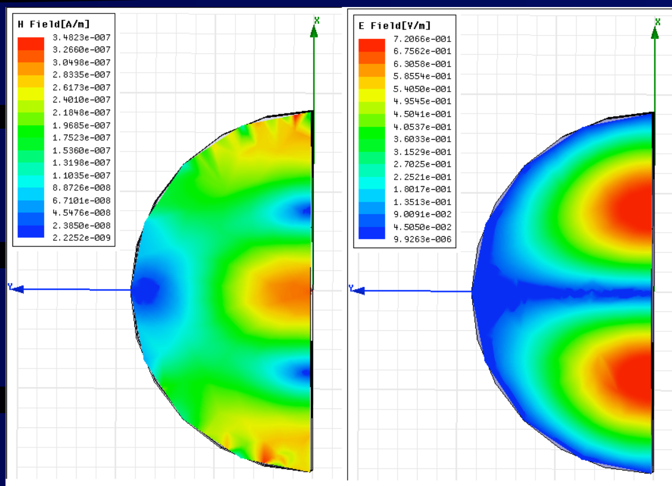

Rods

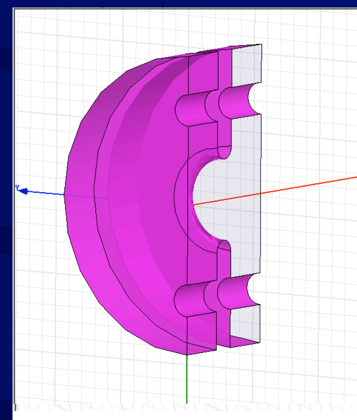

Holes

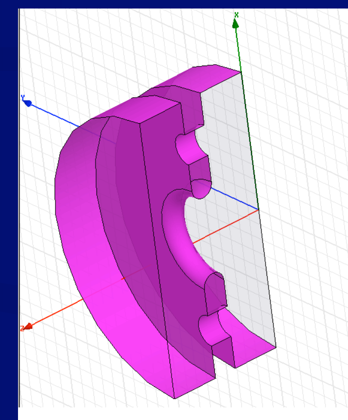

hole/rod radius = 2 mm

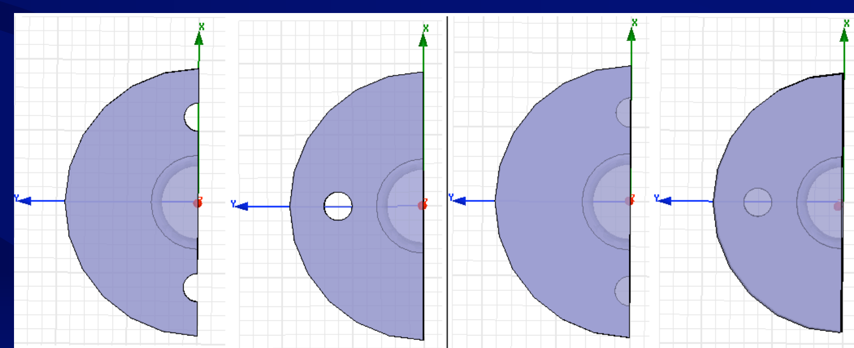

Undesired +1358 MHz | Desired +53 MHz | Undesired -7 MHz | Desired -2 MHz

- Rods give larger mode separation but shift the desired mode too much
- Holes give less mode separation but don't perturb the desired mode.
- In final design, holes used with radius reduced to 1mm, giving a mode separation of 1 MHz.

Final Cavity Design

- 9-cell standing wave structure
- center-fed input RF
- reconditioned VA-24G klystron
- no brazing between cells
- cells are stacked CF vacuum flanges

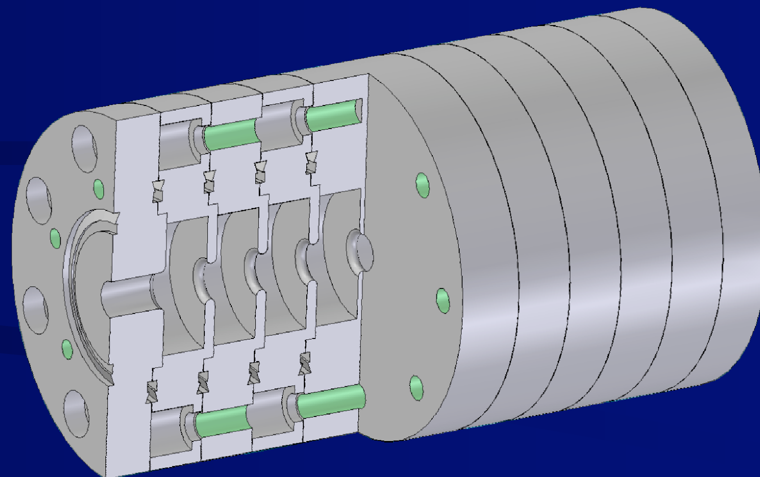

CAD drawing of stacked cells

x-band klystron (50 kW peak)

one cell with polarization holes

S-Band/X-Band RF System

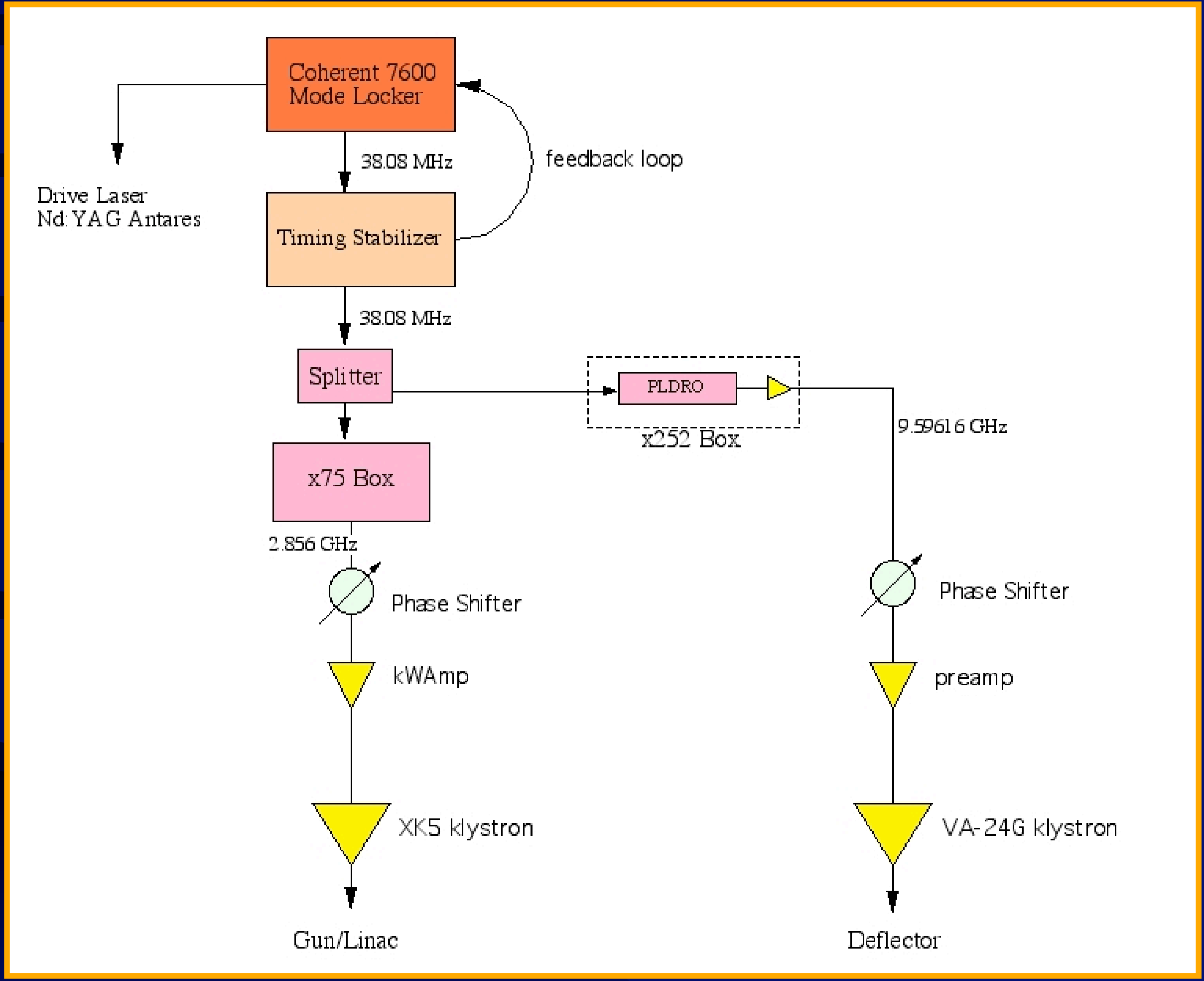

- S and X-Band frequencies are multiples of modelocker freq of drive laser
- Ensures phase stability of gun, linac, laser, and deflector

Bead Pull Results

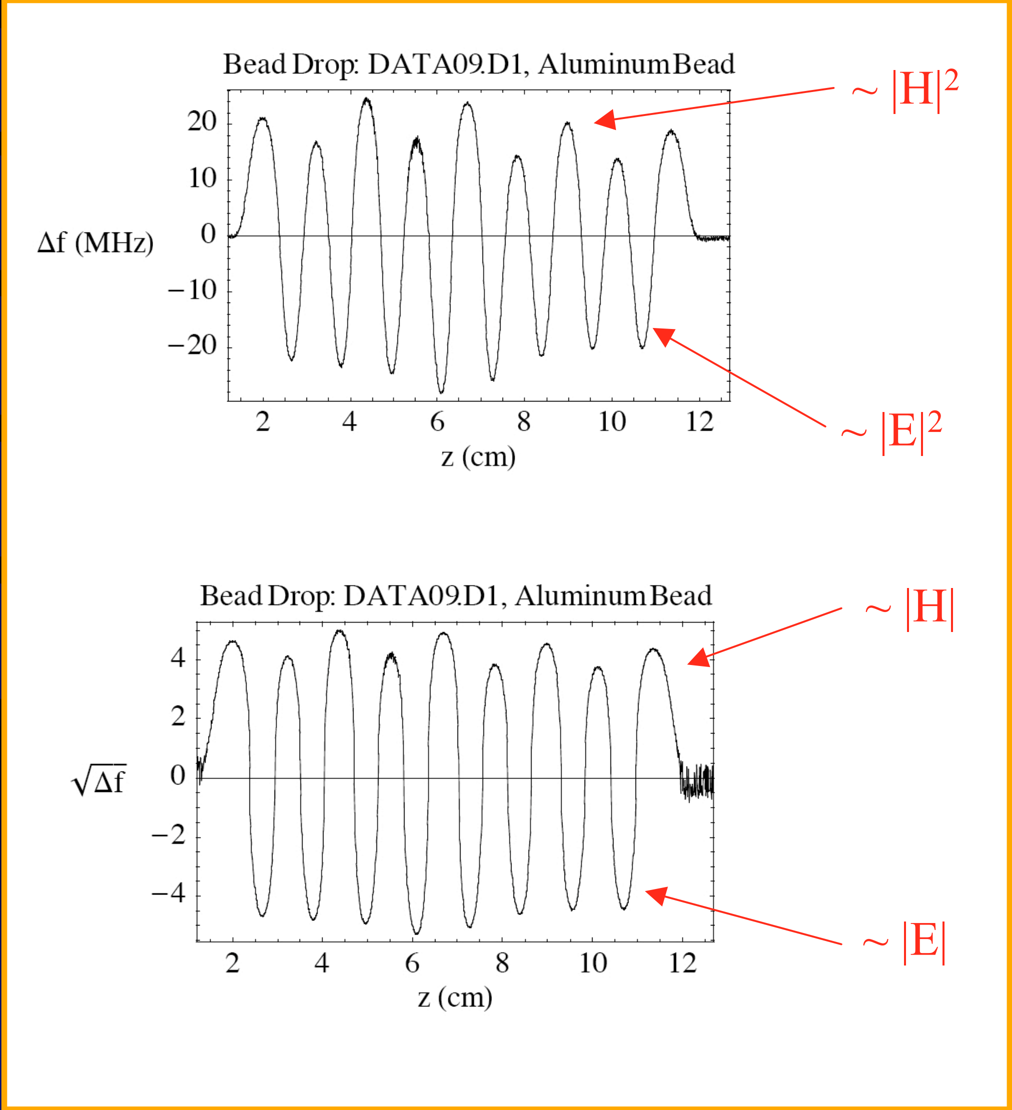

After brazing input coupler

- Bead pull using aluminum bead
- Data proportional to $|E|^2$ and $|H|^2$
- Field flatness ~ ±5%
- Data taken at room temp (24 C)

field flatness ~ 10%

f_0 = 9.60084 GHz ; Δf = 1.5 MHz
β = 0.870 ; VSWR = 1.15
Q_L = 6359 ; Q_0 = 11889 ; Q_e = 13672

Temperature Tuning

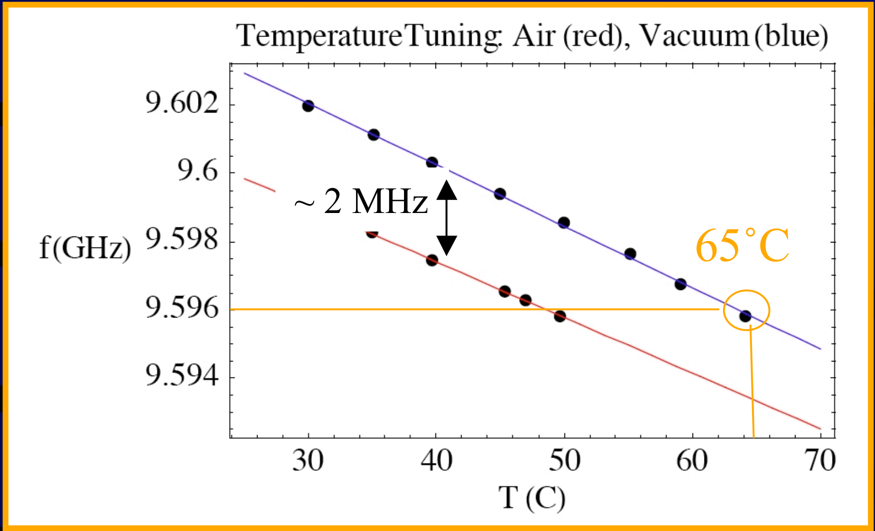

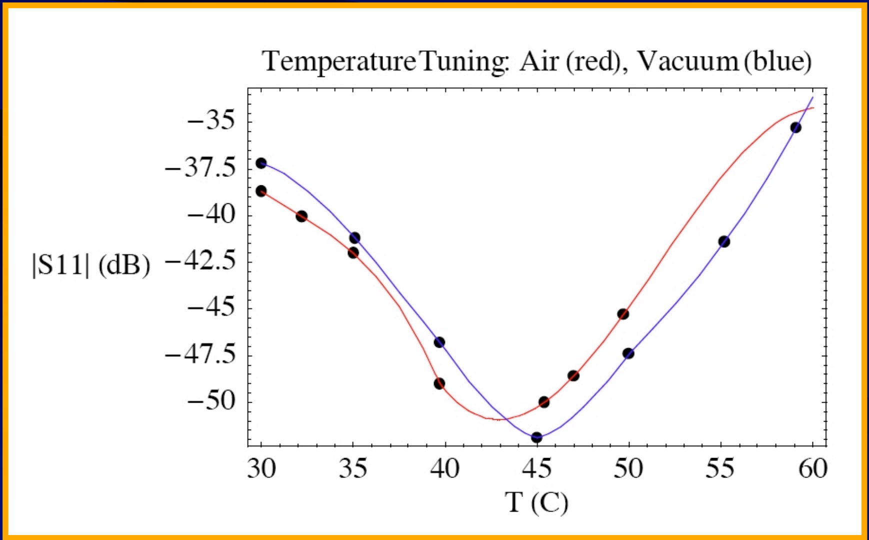

Frequency vs. Temperature

- using heater tape and thermocouple
- PID temperature feedback control
- dots are measured data
- solid lines are linear fits
- d*f*/d*T* = -179 kHz/˚C

f_0 = 9.596 GHz ; Δf = 1.5 MHz
β = 1.036 ; VSWR = 1.03637
Q_L = 6638 ; Q_0 = 13043 ; Q_e = 13517

Reflectance vs. Temperature

- dots are measured data
- solid lines are interpolations
- at optimal freq in vacuum (9.59616 GHz), cavity is slightly overcoupled (-35 dB @ 62 C)
- therefore operating β = 1.036 in vacuum

High Power RF Measurements

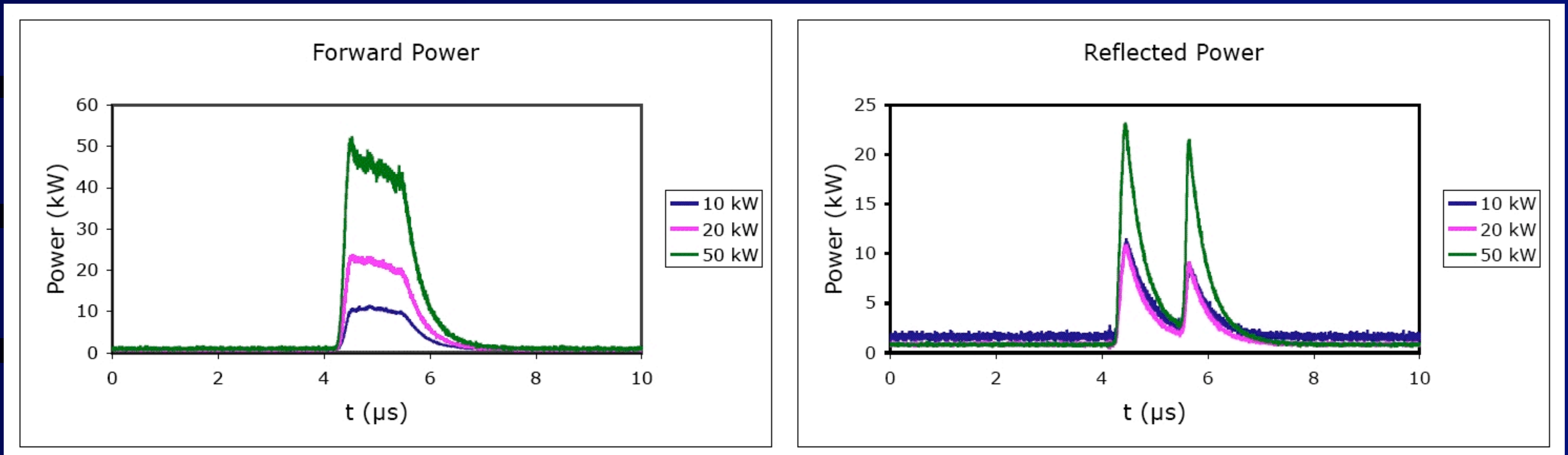

- oscilloscope traces for several attenuation settings
- measured on deflecting cavity waveguide power coupler
- maximum forward power level is 50 kW

Experimental Setup

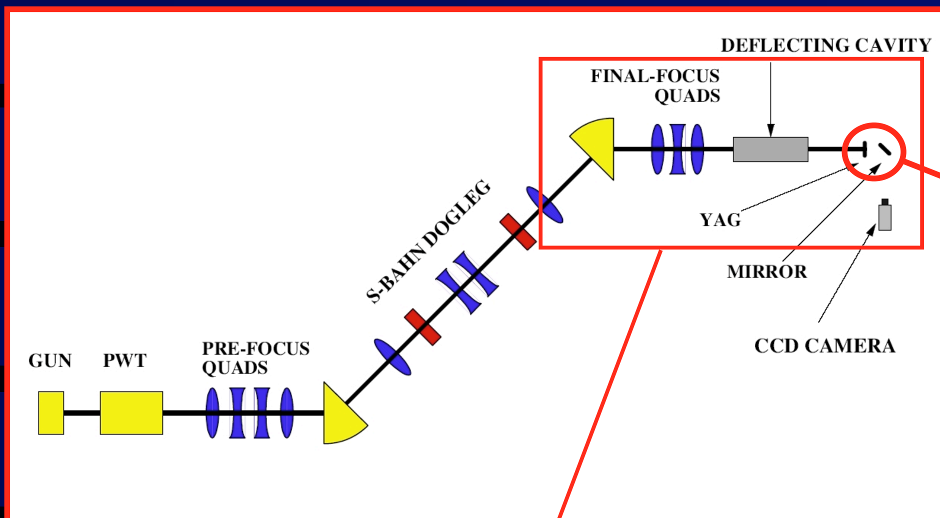

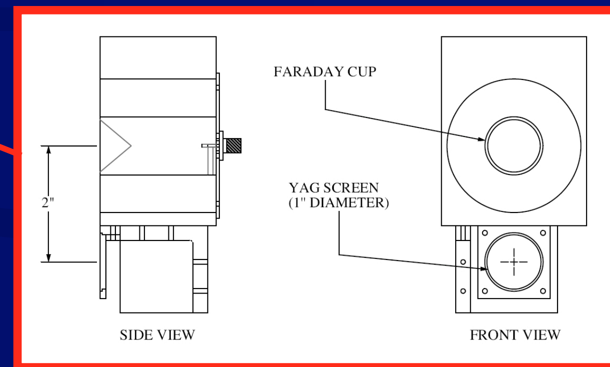

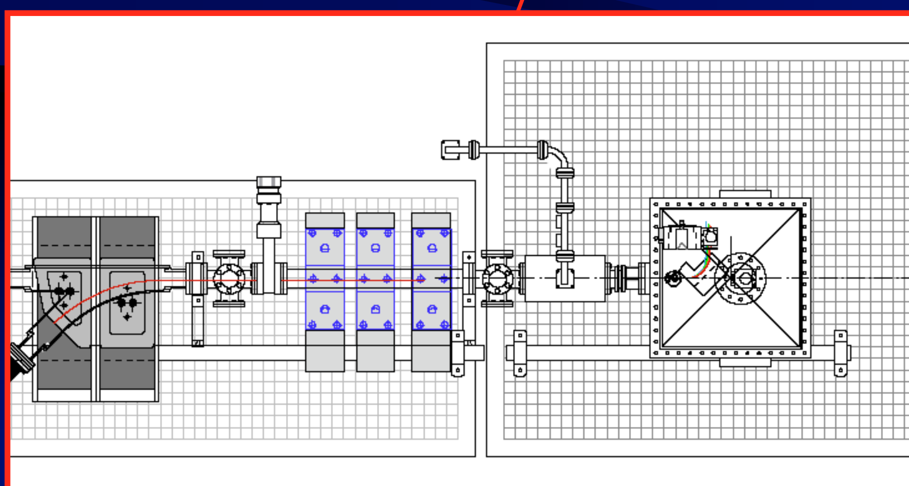

- pop-in faraday cup / 1” YAG
- YAG = ytrium aluminum garnet

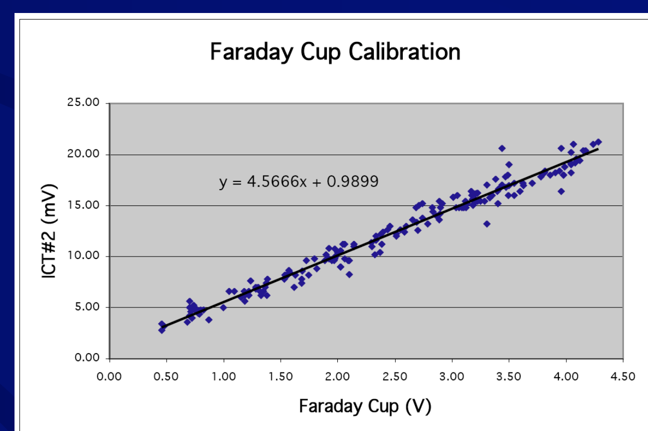

Deflection vs. RF Phase

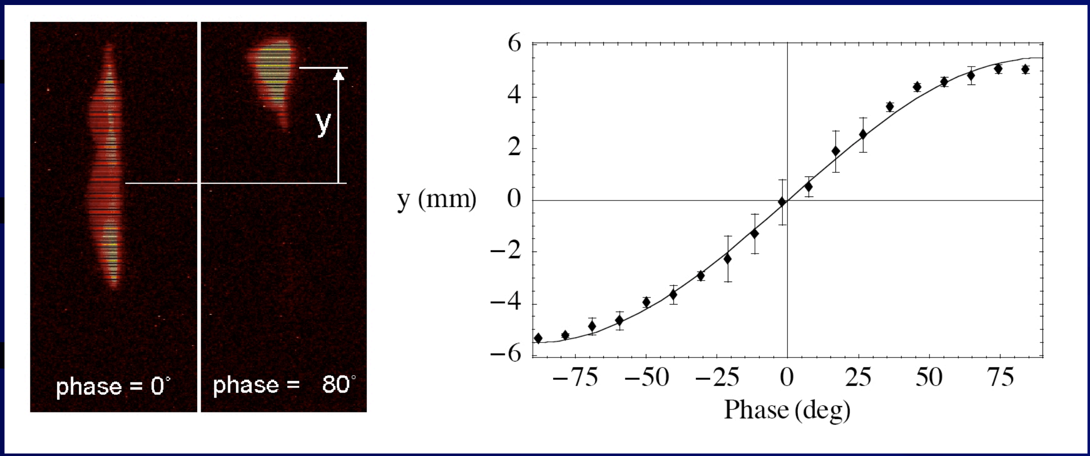

- Solid curve = sine function fit
- Amplitude = eV_0L/p_0c = 5.5 mm

$$y_{cen} = \frac{eV_0L}{p_0c}\sin(\phi_0)$$

Method	Forward Power (kW)	V_0 (kV)
Phase Scan	9.6 kW	232
RF (50 Ω termination)	12.75	267
RF (1 MΩ termination)	12.15	261

- Comparison with RF values
- Calibrated crystal detector
- Assumption: shunt impedance = 5.6 MΩ (sim. value)

Deflecting Cavity: Uncompressed Beam

off on

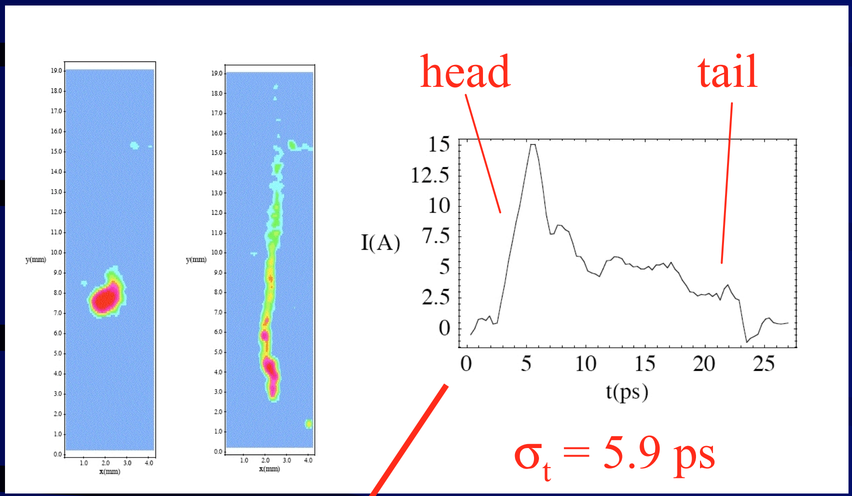

- beam is on-crest in linac (no chirp)
- therefore not compressed in dogleg
- beam appears asymmetrical
- somewhat long pulse
- a lot of structure in the tail
- in some streaks, it is more pronounced
- structure related to nonlinear xtals(?)

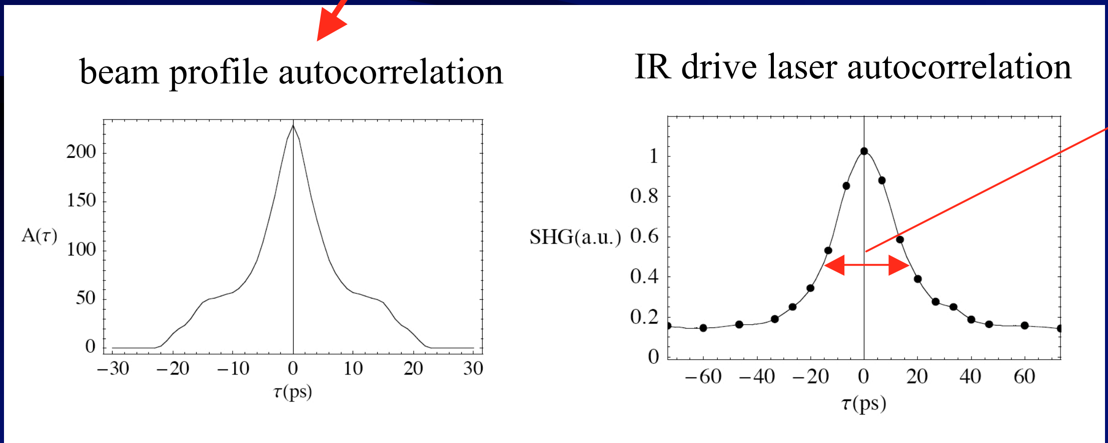

FWHM = 28.8 ps (IR)

doubling xtals
(factor of 2)

FWHM = 14.4 ps (UV)

$\sigma_{rms} \sim 7$ ps

Deflecting Cavity: Compressed Beam

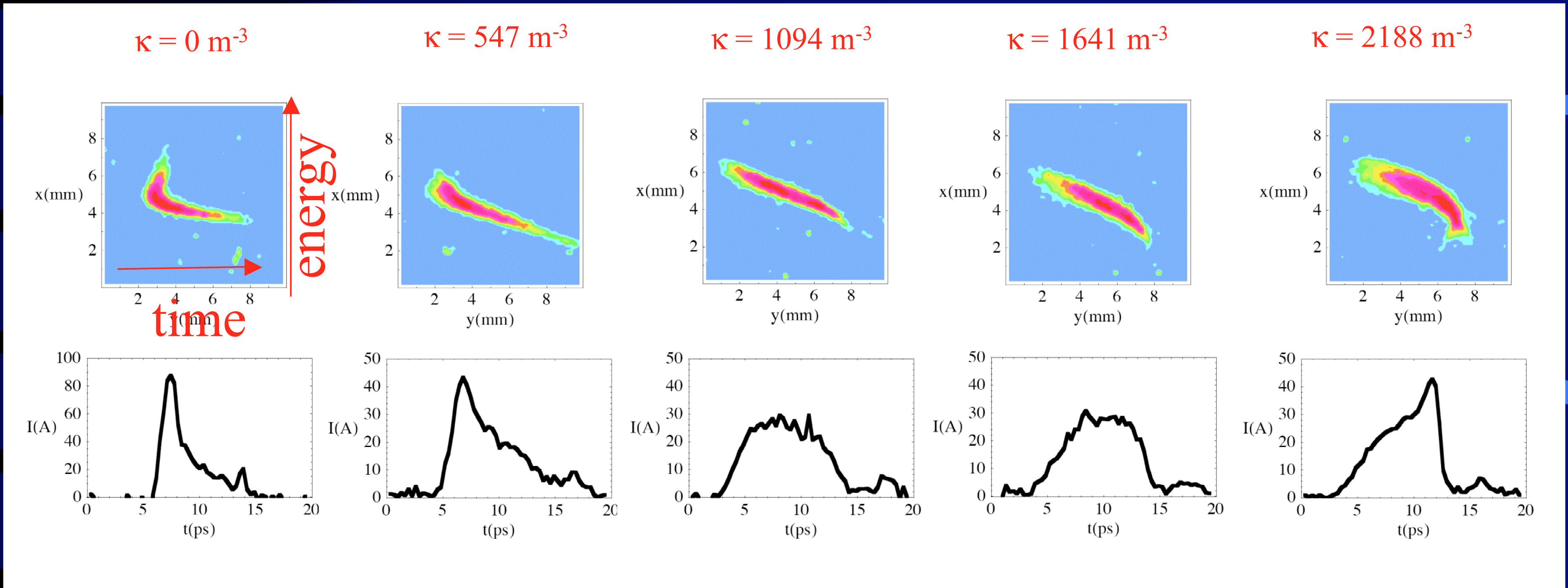

- chirped 20˚ in linac, 234 pC of charge at 11.8 MeV with V_0 = 400 kV
- residual horizontal dispersion produces pseudo-phase space reconstruction
- combination of linear and nonlinear effects (R_{16} & T_{166})
- ramping mechanism clearly visible
- due to asymmetry of initial pulse, overcompensation with sextupoles needed

R. J. England, J. B. Rosenzweig, and G. Travish, PRL **100**, 214802 (2008).

ELEGANT Simulation

“streak” in x,y   z phase space   current profile   “streak” in x,y   z phase space   current profile

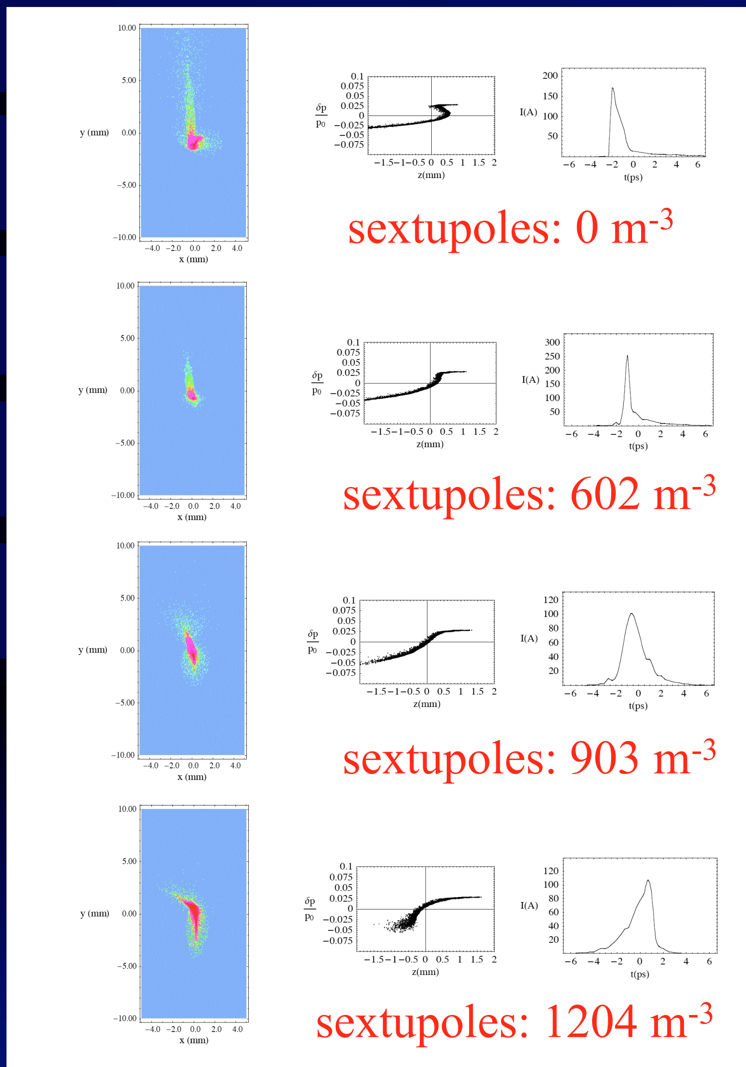

Gaussian beam

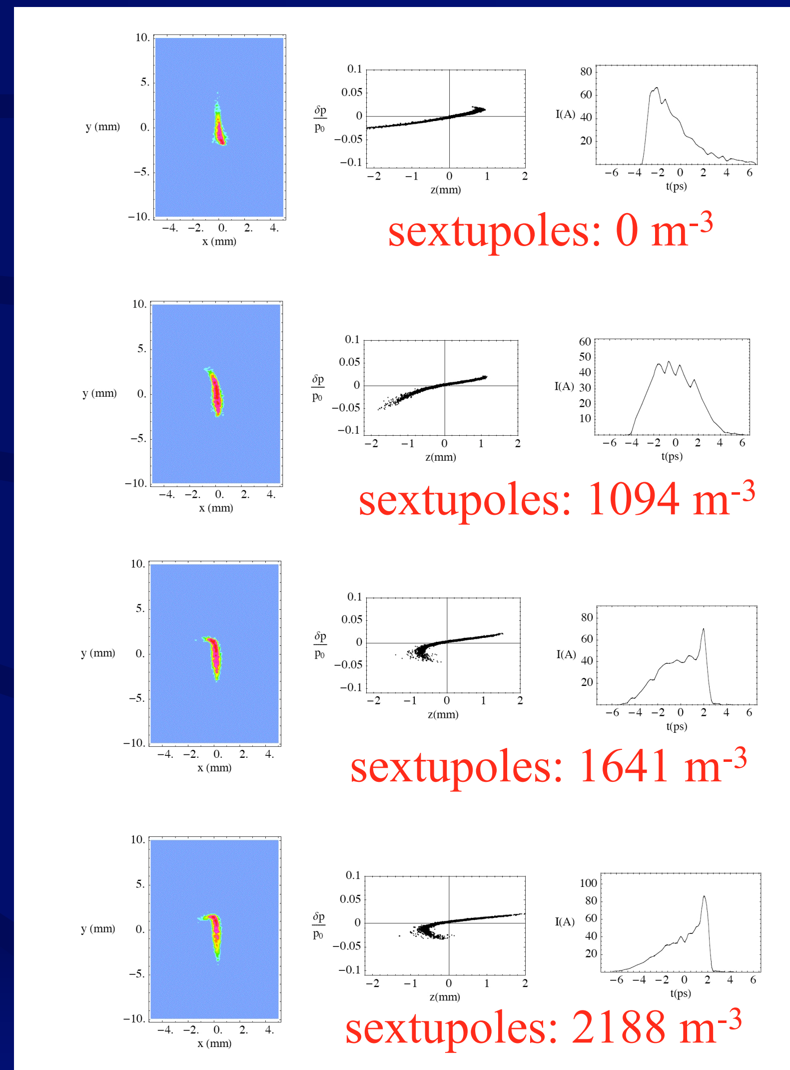

Asymmetric (front-heavy) beam

ELEGANT Simulation

"streak" in x,y　z phase space　current profile　　"streak" in x,y　z phase space　current profile

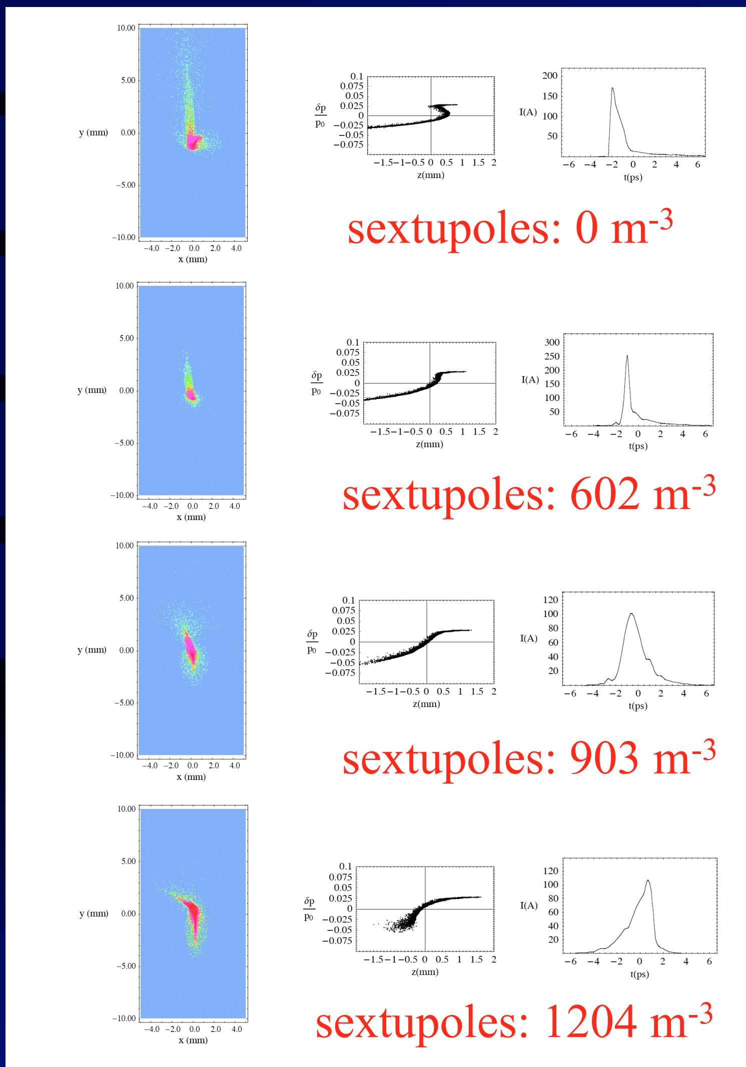

Gaussian beam

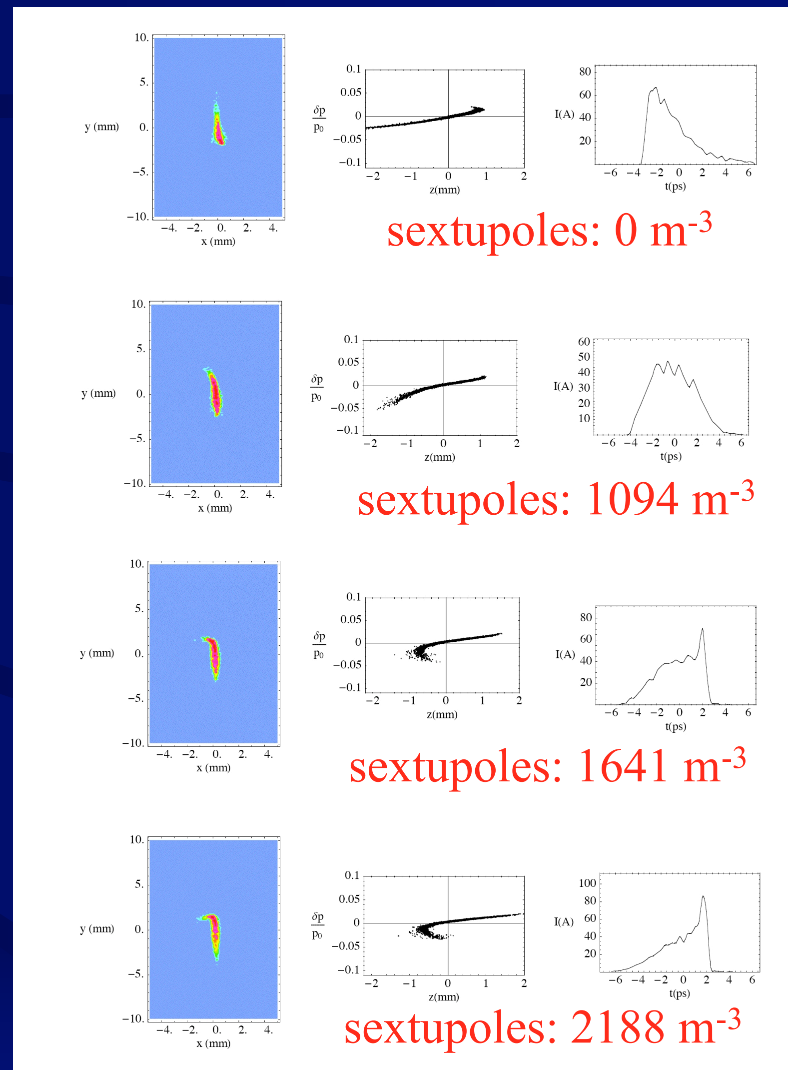

Asymmetric (front-heavy) beam

Future Applications
Witness Beam Generation

For PWFA application, drive beam needs a witness beam to accelerate.

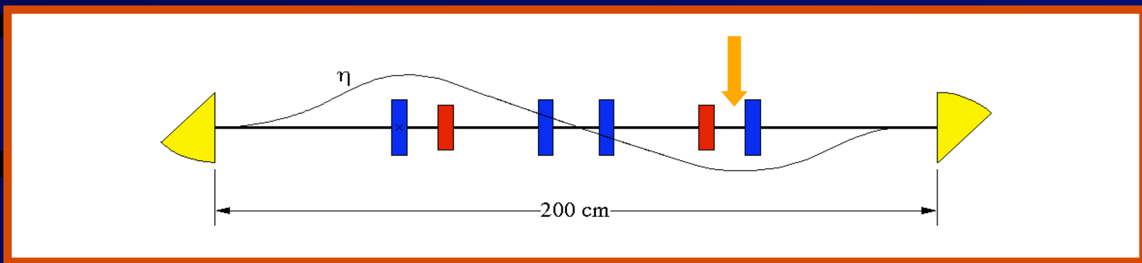

Region of high dispersion in x
Strong correlation b/w x and z
Insert mask in x to **sever** beam in z

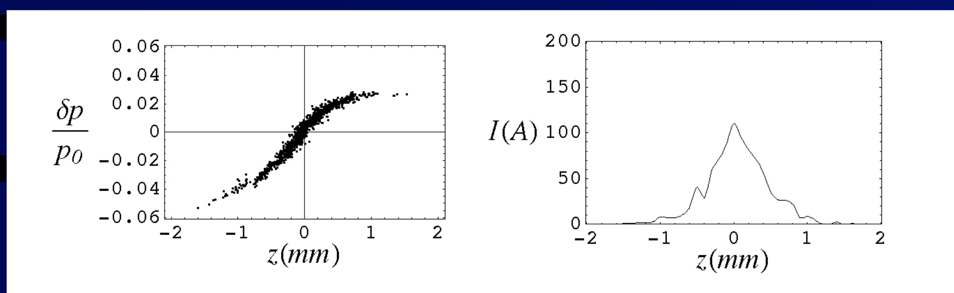

No mask inserted
Undercorrected with sextupoles to elongate profile

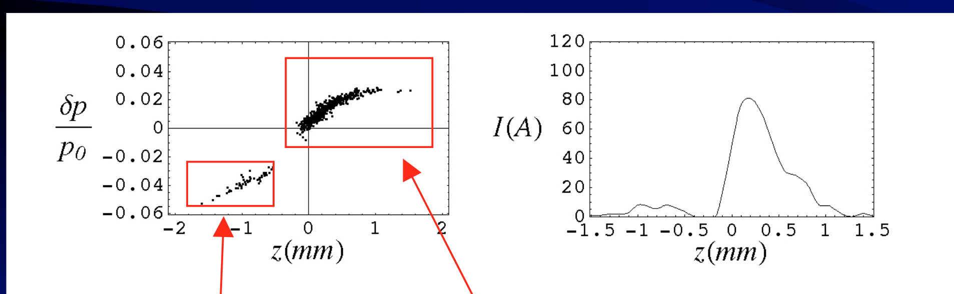

With 1cm mask inserted at above location

witness beam **ramped drive beam**

Future Applications
Tailored Profiles for FACET?

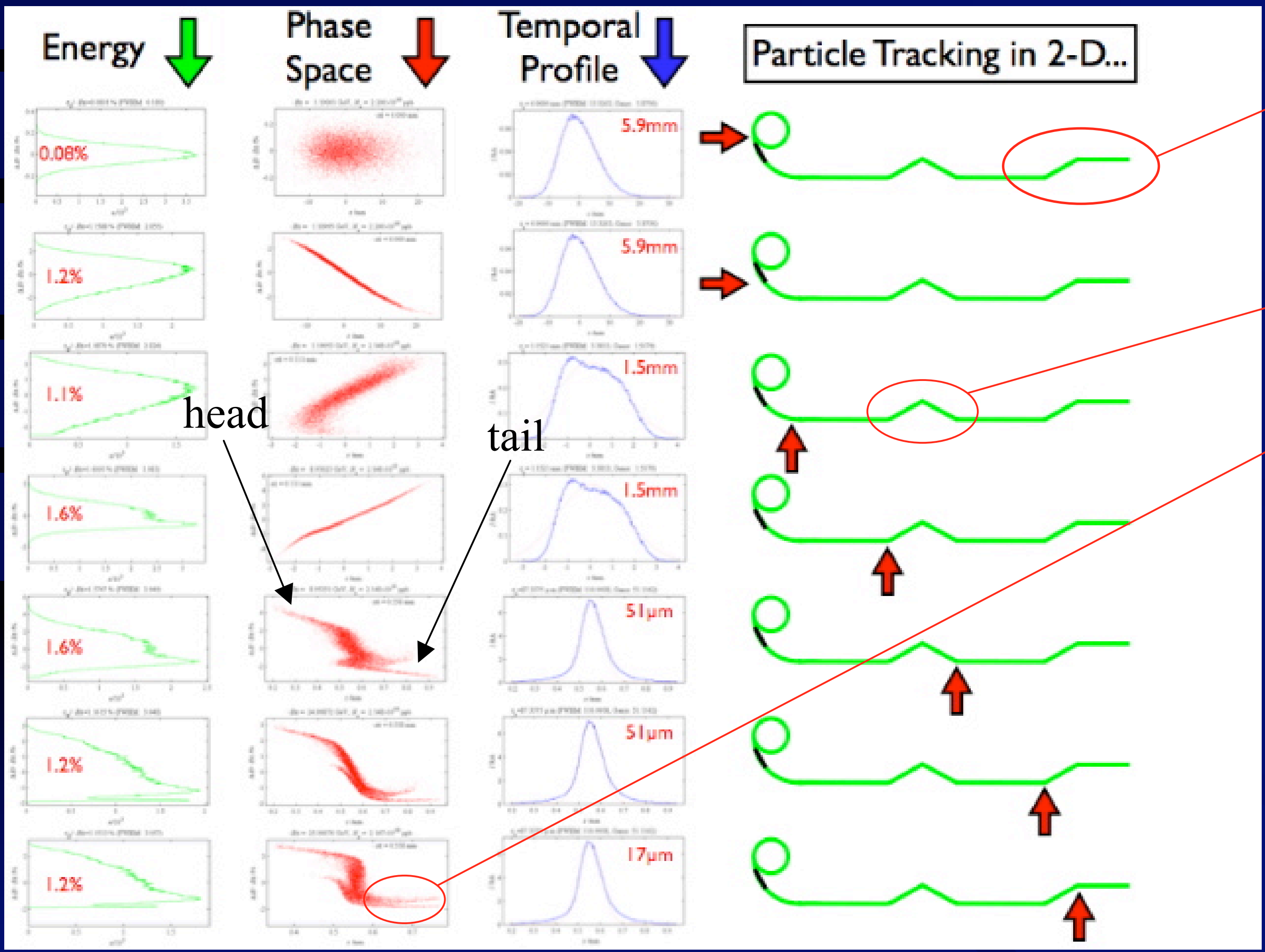

dogleg: R_{56} = -7cm

- reduce chicane compression to increase bunch length to $\sim 2\ k_p^{-1}$
- collimate to remove low-energy tail

Conclusions

- Proposal:
  - ramped beams: improved transformer ratio (R > 2) for PWFA applications
  - feasible using dogleg compression with sextupoles
  - deflecting cavity diagnostic (500 fs resolution)
- Deflecting cavity
  - final cavity design finalized in 3-phase process w/ 2 prototypes
  - cavity testing indicates that it operates within the design specifications
  - high power RF testing: no breakdown problems observed
- Experimental tests:
  - unchirped (uncompressed) beam has asymmetric structure
  - chirped beam w/residual dispersion = semi-tomographic reconstruction
  - evidence for ramp-shaped electron beams
- Other Experiments:
  - deflector use for measuring optimized charge distributions
  - dogleg high-brightness focus studies
  - witness bunch generation

Acknowledgements

Laser-Plasma Group

Chan Joshi
Sergei Tochitsky
Jay Sung
Chris Clayton

UCLA Physics Staff

Christine Green
Harry Lockart
Jim Kolonko
Teresa Wheeler
Penny Lucky

UCLA Particle Beam Physics Lab

James Rosenzweig
Brendan O'Shea
Joris Fourrier
Claudio Pellegrini
Pietro Musumeci
Oliver Williams
Matt Thomson
Scott Anderson
Rodney Yoder
Pedro Frigola
Gerard Andonian
Alan Cook
Mike Dunning
.... and many more

Introduction: The RF Photoinjector

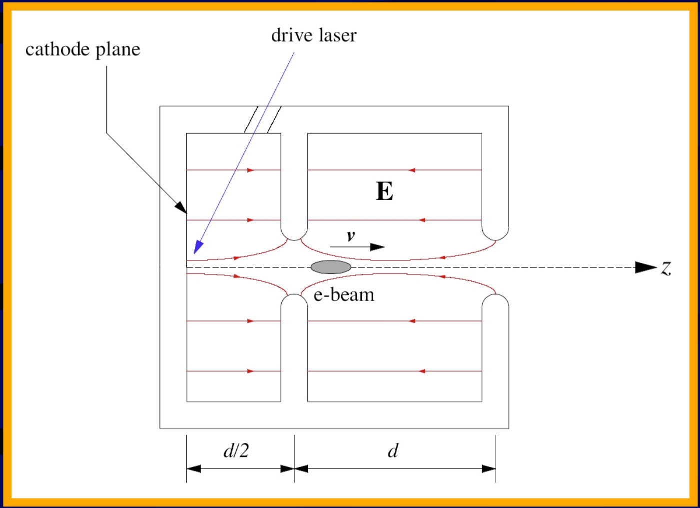

- Acceleration from rest to relativistic energies (~ 1 to 10 MeV)
- Temporal structure of electron beam reflects that of laser pulse on the cathode.
- Capable of producing low-emittance beams.
- Emittance: figure of merit; measure of area occupied by beam distribution in transverse phase space.

$$\varepsilon_{x,N} = \frac{1}{mc}\sqrt{\left\langle p_x^2 x^2 \right\rangle - \left\langle p_x x \right\rangle^2} \approx \sqrt{\varepsilon_{x,th}^2 + \varepsilon_{x,rf}^2 + \varepsilon_{x,sc}^2}$$

thermal emittance: $\varepsilon_{x,th} \propto \sigma_x$

RF emittance: $\varepsilon_{x,rf} \propto \sigma_x^2 \sigma_z^2$

space charge emittance: $\varepsilon_{x,sc} \propto \dfrac{1}{\sigma_z}$

- Trade-off between rf and sc components
- Implies optimal pulse length σ_z.
- Generally determined by photoinjector codes (e.g. PARMELA, HOMDYN)
- Typical σ_z ~ 10 degrees of RF phase
- For S-Band (2.856 GHz) 10 deg ~ 10 ps

Beam Brightness

$$B_\perp = \frac{I}{\varepsilon_{x,N}^2} \qquad I \propto \frac{Q}{\sigma_z}$$

$$Q_{\max} \approx \frac{2}{5}\pi\sigma_x^2\varepsilon_0 E_0$$

- "brightness": measure of density of particles in transverse phase space.
- emittance constrained by photoinjector: $\varepsilon_N > 1\ \mu$m
- σ_z constrained (~ 10 deg of RF phase) to minimize ε_N
- Q constrained by cathode image charge limit

Rosenzweig, Colby, AIP Conference Proc. 334, p. 724-737 (1995).

- optimal photoinjector brightness
- to obtain higher brightness beams, require compression techniques

$$B_{\perp,opt} = 16(2\pi)^{9/2}\alpha k \frac{I_A[1+\frac{3}{5}A]^2}{\sigma_z A^2}$$

α=1.5; λ=10cm; A=1; I_A=16kA; σ_z=3mm

$$B_{\perp,opt} = 80\ \text{A}/\mu\text{m}^2$$

Bunch Compression Techniques

RF Techniques

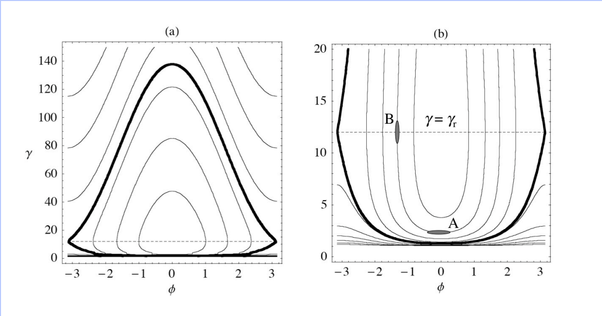

Phase Space Rotation

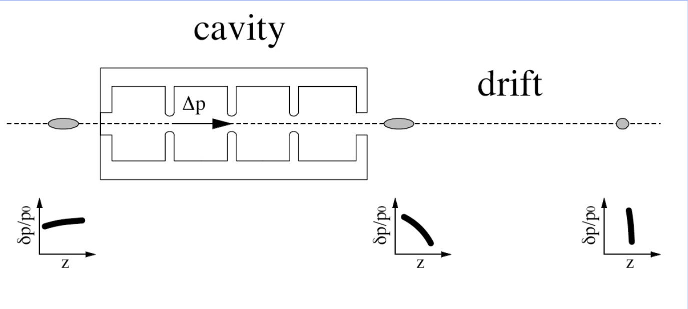

Ballistic Compression

Magnetic Techniques

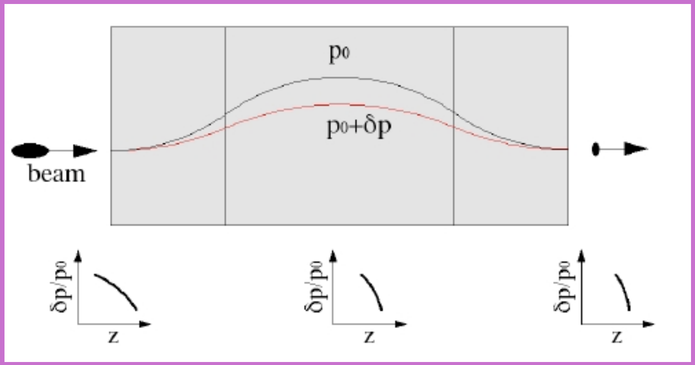

Chicane

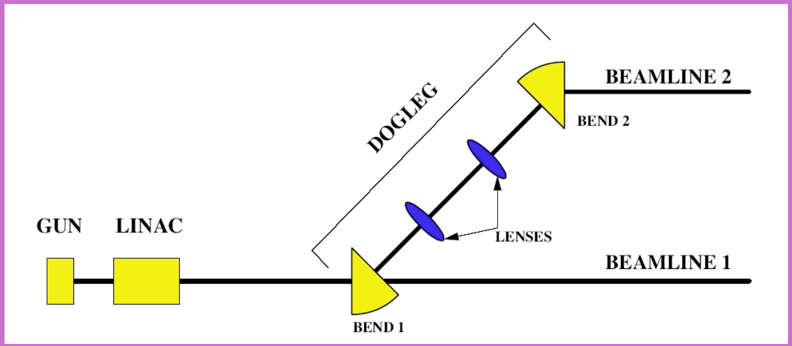

Other Nonisochronous Devices
(e.g. dogleg compressor)

Applications for High Brightness Beams

Free electron laser

- high gain regime
- minimize the gain length L_g

$$L_g = \frac{\lambda_u}{2\sqrt{3}\pi\rho} \qquad \rho \propto \omega_p^{2/3} \propto n_e^{1/3}$$

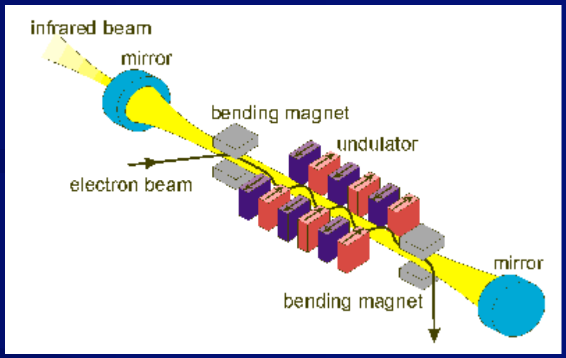

Inverse Compton Scattering

- beam + laser (hν) ---> higher hν‘ photons
- shortness of scattered pulse limited by shortest of beam, laser

$$N_{ph} = \mathcal{L}\sigma_T \qquad \mathcal{L} \propto \frac{N_e}{A_{\text{int}}}$$

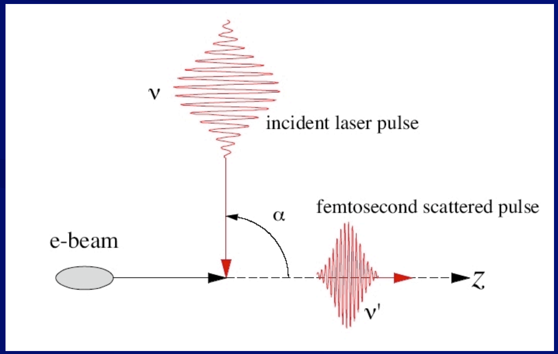

Plasma Wakefield Accelerator:

- beam + plasma --> high-gradient wakes
- beam density, time profile important

$$E_{\max} = E_0 1.3\Lambda \ln(1/\sqrt{\Lambda/10}) \qquad n_{\text{beam}} >> n_0$$

$$\Lambda = (n_{beam}/n_0)k_p^2\sigma_r^2$$

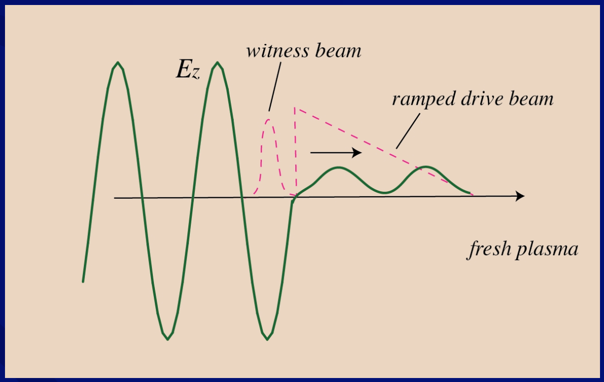

Further Applications: Deflecting Cavity

Dynamically Optimized Beam Profiles

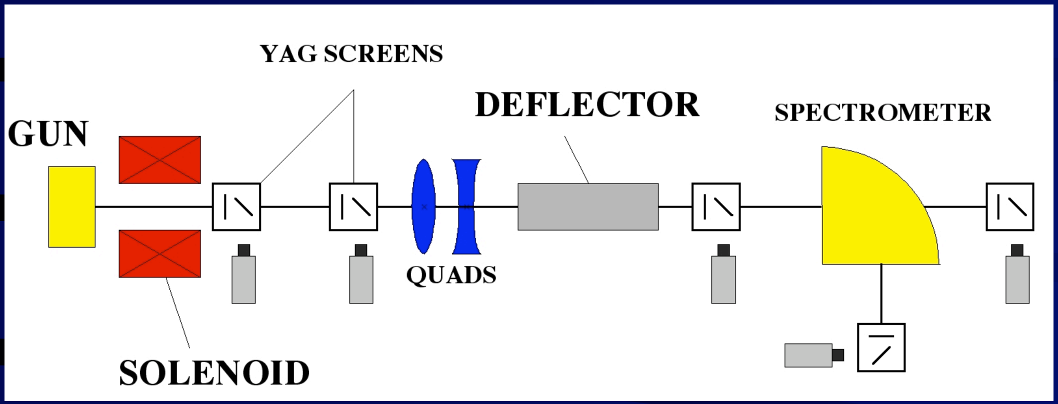

Beam Charge:	0 to 50 pC
Beam energy:	up to 4 MeV
Power Source:	18 MW Klystron
RF Frequency:	2.856 GHz (S-Band)
Cathode laser:	10 μJ at λ = 266 nm
Laser pulse length:	50 fs RMS

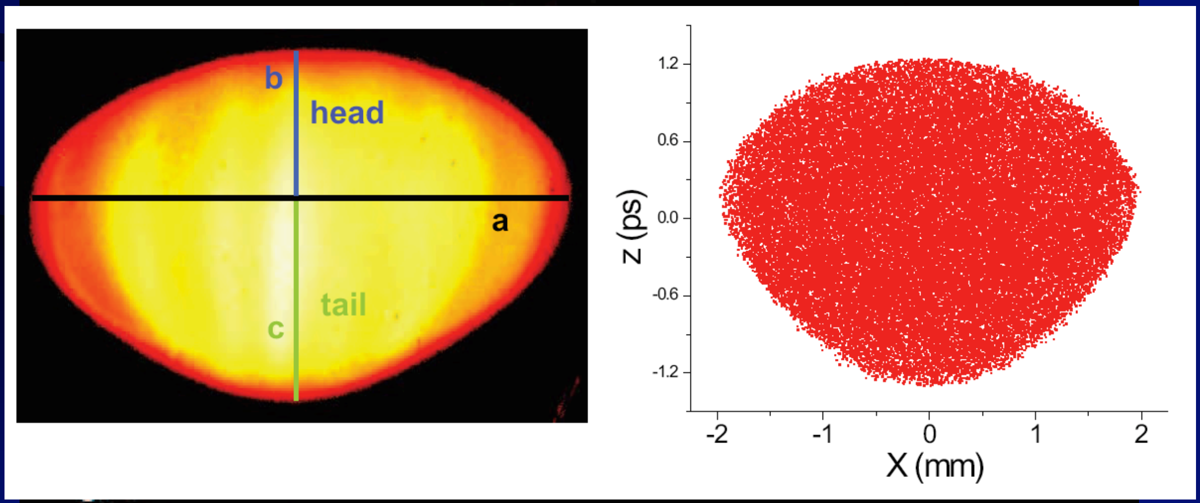

P. Musumeci, J. T. Moody, R. J. England, J. B. Rosenzweig,T. Tran "Experimental generation and characterization of uniformly filled ellipsoidal beam distributions," (submitted to PRL).

Further Applications: Doglegs

BNL - VISA I

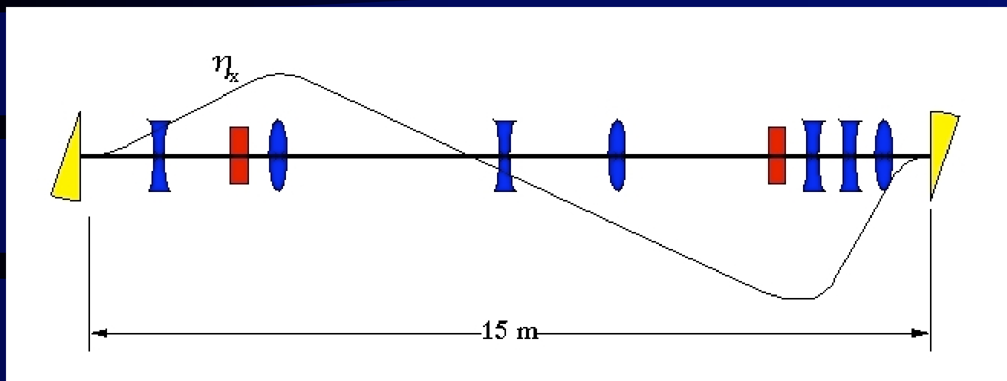

- observed compression when running off-energy by 0.76%
- however, for negative chirp, dogleg should expand, not compress

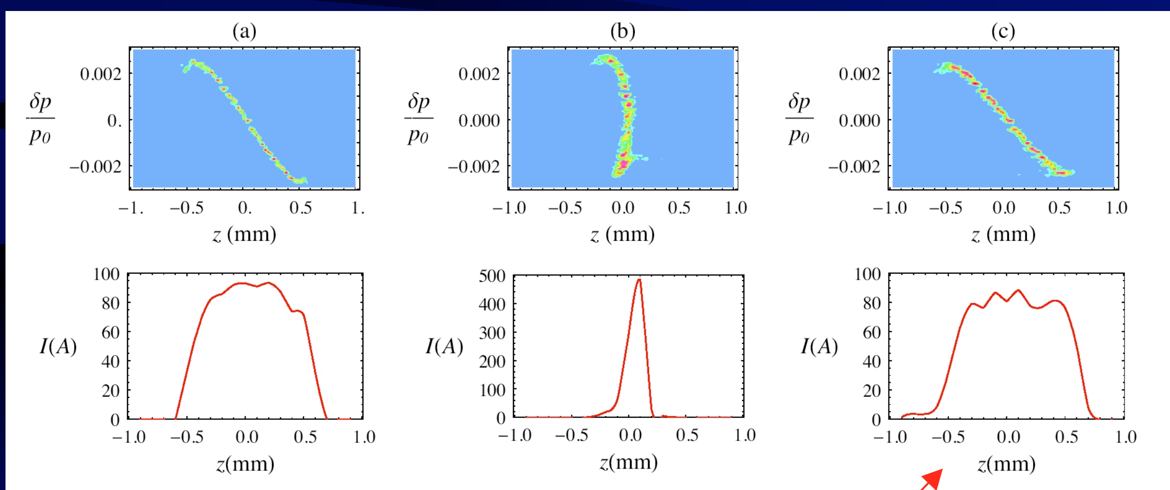

-0.4 cm

-10m (!)

$$z_f = z_0 + R_{56}\delta + T_{566}\delta^2$$

off energy by Δ = -0.76%

$$\hat{R}_{56} \simeq R_{56} + 2T_{566}\Delta$$

$$z_f = z_0 + \hat{R}_{56}\hat{\delta} + \hat{T}_{566}\hat{\delta}^2$$

+18 cm

sextupoles used to remove T_{566}

R. J. England, et. al. "Sextupole correction of the longitudinal transport of relativistic beams in dispersionless translating sections," PR-STAB **8**, 012801 (2005).

Further Applications: Doglegs

SLAC - ORION Low-E Hall Dogleg

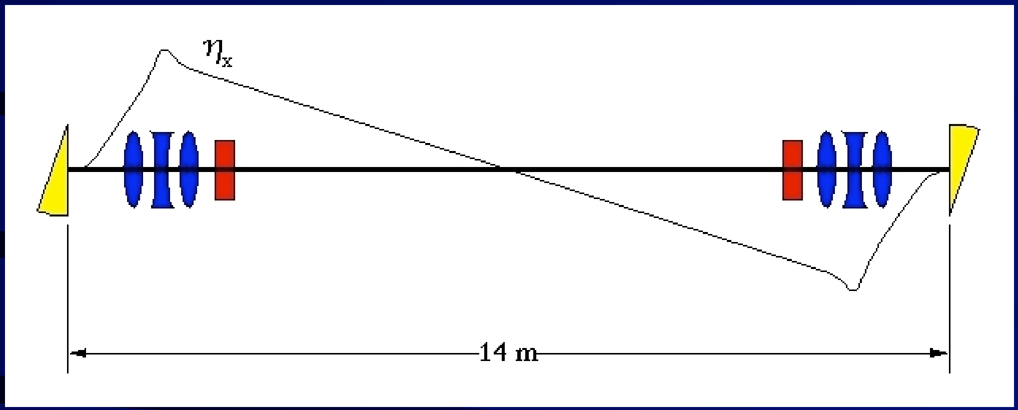

- studies for PWFA / general transport
- large energy spread requires octupole correction

initial beam | no sextupoles | with sextupoles | sext's + oct's

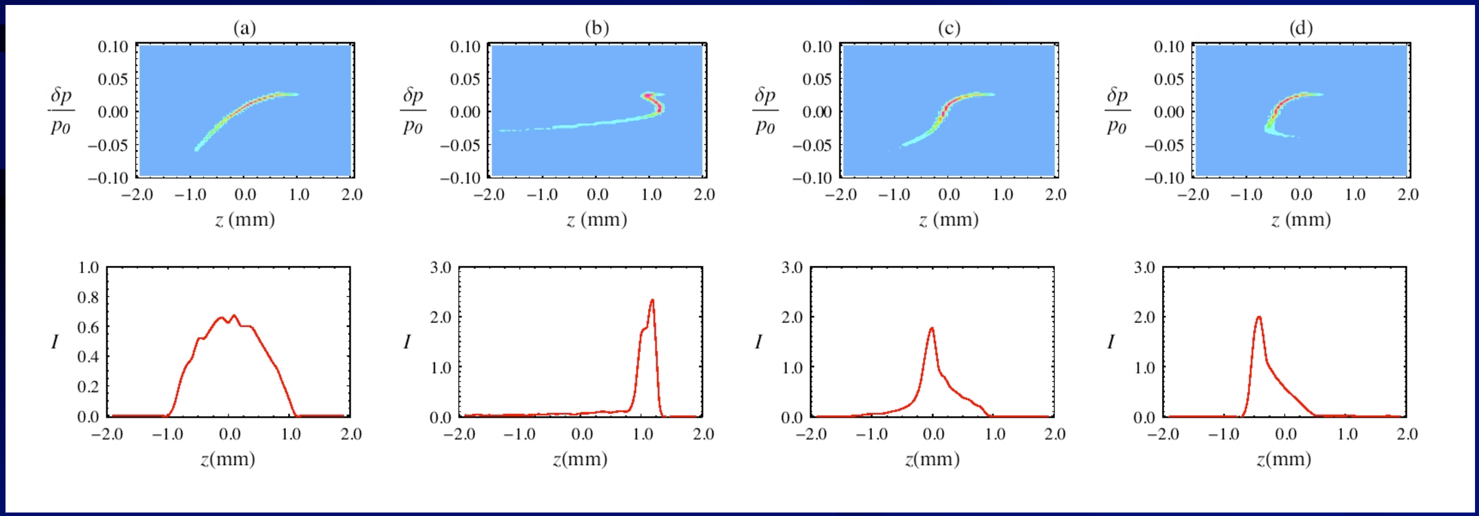

R. J. England, et. al. "Sextupole correction of the longitudinal transport of relativistic beams in dispersionless translating sections," PR-STAB **8**, 012801 (2005).

Future Experiments

PMQ Focusing

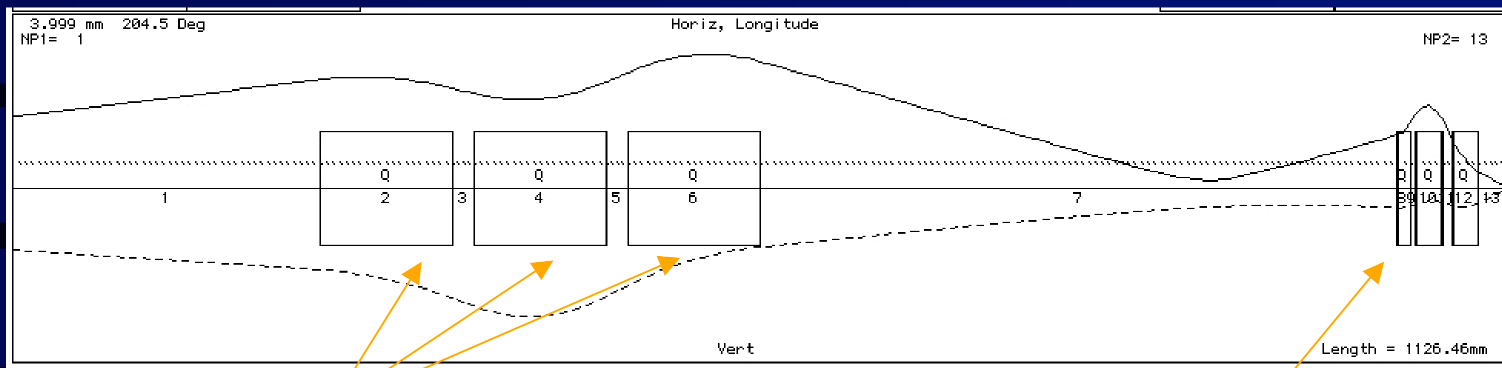

standard iron quads

PowerTrace 1.08 Simulation

PMQs (110 T/m)

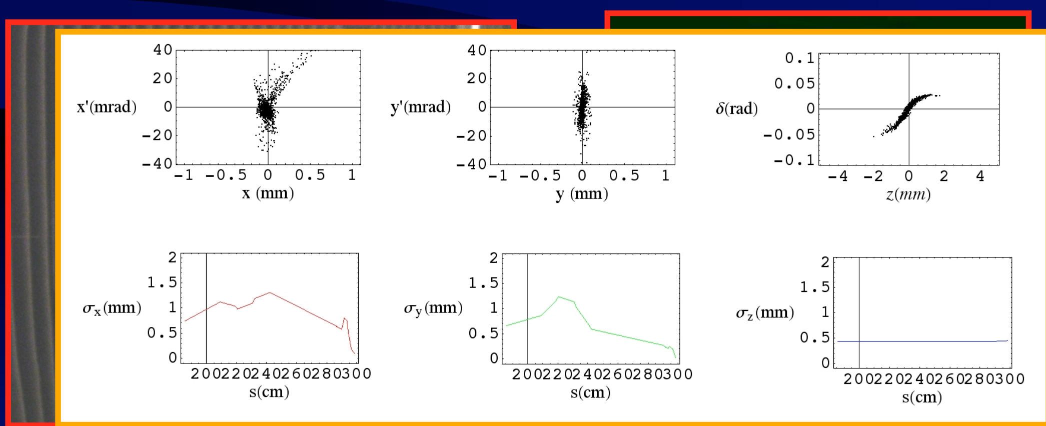

- ELEGANT Simulation Result
- γ=25.7; E=13.13 MeV; Q = 300 pC
- σ_x=130 μm; ε_x=41 mm mrad
- σ_y=57 μm; ε_y=18 mm mrad
- σ_z=0.51 mm; σ_δ=1.84%

- Hybrid Permanent Magnet and Iron
- Grey cubes are Alnico; M=1.175 T
- Field gradient: B'=310 T/m; B''=0.002 T/m^2
- Bore diameter = 8mm
- Benefits: cheaper, better field profile
- Downsides: small bore; in-vacuum

$$\mathcal{B} \simeq \frac{2Q/\sigma_t}{\varepsilon_{N,x}\varepsilon_{N,y}} = 412 mA/\mu m^2$$